AD 262 843

AVCO RESEARCH LABORATORY

PHYSICAL GAS DYNAMICS RESEARCH AT THE AVCO RESEARCH LABORATORY

by

P. H. Rose

a unit of the RESEARCH and ADVANCED DEVELOPMENT DIVISION

Research Report 9
Formerly
Research Note - 37
May, 1957

AVCO RESEARCH LABORATORY
Everett, Massachusetts U. S. A.

a unit of

RESEARCH AND ADVANCED DEVELOPMENT DIVISION
AVCO MANUFACTURING CORPORATION

PHYSICAL GAS DYNAMICS RESEARCH AT THE AVCO RESEARCH LABORATORY*

by

P. H. ROSE**

Presented at the 7th Meeting of the AGARD Wind Tunnel and Model Testing Panel in July, 1957 at Scheveningen, Netherlands.

* AVCO Research Laboratory Research Report 9
** Principal Research Scientist

ABSTRACT

A resume of the work of the AVCO Research Laboratory during essentially the first year of its existence in the field of high temperature gas dynamics is presented. This laboratory was organized early in 1955 by Dr. Arthur Kantrowitz to investigate the physical gas dynamic problems associated with the high temperatures involved in flight at hypersonic Mach numbers. The central concept of this work is that the important elements of the environment anticipated could be duplicated in shock tubes.

The advantages of the straight shock tube for investigation of high temperature gas dynamics are discussed. For many phenomena, such as boundary layer problems (other than transition), the parameters important in classical, low temperature aerodynamics, such as Mach number and Reynolds number, are shown to lose much of their importance in the high temperature, dissociating gas, situation. Instead, the flow chemistry is shown to be a critical simulation parameter. The kinetics of the flow chemistry are simulated if the enthalpy and pressure of the gas are reproduced.

The enthalpy and pressure attainable at the stagnation point of a blunt model in a shock tube are given and are shown to duplicate those encountered at the stagnation point in flight up to the satellite velocity. In addition the condition in the hot gas behind both the moving shock wave and behind a shock wave reflected from the closed end of the tube are shown to be applicable to the study of many hypersonic flight phenomena.

Several investigations, conducted in shock tubes, into critical gas dynamic problems associated with the high temperature are described. Heat transfer measurements in the laminar, dissociated, boundary layer at the stagnation point are discussed. Measurements of the radiative emissivity and electrical conductivity of high temperature air are described. Other investigations into the properties of high temperature gases, including preliminary studies of magnetohydrodynamics are summarized.

INTRODUCTION

At a previous meeting of the AGARD Wind Tunnel and Model Testing Panel in Paris the shock tube as a high temperature aerodynamic research and development tool was discussed by Colonel Dodge[1]. Much of the discussion centered about ways of producing hypersonic Mach numbers to completely simulate the flight environment. More recently in Ottawa, Dr. Kantrowitz[8] addressed this group and outlined a program designed to answer many of the problems of high temperature hypersonic gas dynamics by the use of straight shock tubes without high Mach number nozzles, and within the state of shock tube technology as it then existed.

Since early 1955, the AVCO Research Laboratory has been working on implementing this program under the direction of Dr. Kantrowitz. The work of this group, over essentially the first year of its existence, will be reported in this paper. It has been our philosophy in this research not to attempt to develop a facility with the maximum flexibility for investigating hypersonic problems, but to consider specific areas and design apparatus which could be quickly constructed and which through theoretical analysis and experimental verification may shed some light on high temperature phenomena.

The relative kinetic energy of the air intercepted by a hypersonic vehicle flying at the satellite velocity is large enough to dissociate all the oxygen molecules into atoms, dissociate about half of the nitrogen, and thermally ionize a considerable fraction of the air. The presence of free-atoms, electrons, and molecules in excited states can be expected to complicate heat transfer through the boundary layer by additional modes of energy transport such as atom diffusion carrying the energy of dissociation. Radiation by transition from excited energy states may contribute materially to radiative heat transfer. There is also a possibility of heat transfer by electrons and ions. The existence of large amounts of energy in any of these forms will undoubtedly influence the familiar flow phenomena.

Exploration of the relationship between the high temperature phenomena and gas dynamics requires careful consideration of both the environment and the problem, because the usual, non-dissociating gas, aerodynamic parameters are not necessarily required for simulation. Aerodynamic heat transfer, like other boundary layer problems, does not require the simulation of Mach number ahead of

the bow shock so long as the pressure distribution is similar in the test and flight situations*. This can easily be seen by considering the boundary conditions for the boundary layer. In the shock tube one can simulate the stagnation enthalpy and pressure. Thus, if the pressure distribution is the same in flight and shock tube, the absolute values of the gas properties at every point outside the boundary layer are identical for the two cases if thermodynamic equilibrium exists. For boundary layer problems simulation is thus complete in equilibrium, but are departures from equilibrium identical? In the shock tube the incident shock may leave the air in a non-equilibrium state, i.e., partially dissociated. However, as the air passes through the bow shock at the nose of a model it is immediately raised to a very high temperature where dissociation proceeds very rapidly. The high temperature will effectively erase any memory of the gas state upstream from the shock wave, since dissociation will proceed very rapidly until the translational temperature is reduced to a value low enough to slow up the reaction rate. Thereafter the chemical state of the gas is determined by the pressure time history. This depends only on the initial state and the pressure distribution, which are both reproduced in the shock tube. The chemical state is therefore simulated correctly at every point.

However, in a dissociated gas in a realistic shock tube, the model size must be different from the flight vehicle, and, because the degree of dissociation depends on both temperature and pressure, the pressure and model size cannot be used to compensate each other as, for instance, Reynolds No. simulation in classical aerodynamics. Thus both Reynolds number and Mach number lose some of their significance as simulation parameters.

Realization of this fact eliminates one of the most important difficulties in the application of the shock tube to hypersonic aerodynamics. Complete simulation is theoretically possible in shock tubes by the use of the expansion nozzles but demands

---

* It will be shown in a later section that for certain blunt bodies, such as a hemisphere-cylinder, the shock tube pressure distribution is Newtonian and therefore identical to the estimated flight pressure distribution at Mach three or more. As a result, the pressure distribution simulation is independent of Mach numbers.

excessive driver pressures and nozzle expansion ratios of the order of 10^6. However, when the large total pressure loss across a high Mach number bow shock is eliminated, as in the straight shock tube, the smaller degree of irreversibility allows stagnation pressures and pressure distributions typical of many hypersonic flight situations to be achieved.

For radiation studies shock tube simulation is more obvious. It has been stated that the thermochemical state of the air is correctly reproduced in the shock tube. However, the thickness of the hot gas region is much smaller and the conversion to flight must be made by geometric consideration of the two cases.

Like radiation, other physical gas properties can be studied in the known state of the hot gas in the shock tube, and consequently applied to the flight situation

Based on this philosophy, the staff of the AVCO Research Laboratory have investigated many of the critical questions of hypersonic flight and, through exploitation of the straight shock tube, have obtained engineering answers which are being used for design and development of hypersonic vehicles[30]. The research we have conducted has been aimed at answering the most critical questions, i.e.; (1) Can we learn enough about the chemical kinetics of the high temperature air and component gases to define the thermodynamic state in both the shock tube and flight; (2) Is the aerodynamic heat transfer, as determined from a laminar boundary layer theory including diffusion of atoms, a good approximation to the high temperature situation or are there unanticipated phenomena present; (3) What is the radiative emissivity of high temperature air; and (4) Do the other high temperature gas properties, such as the electrical conductivity, complicate hypersonic flight?

The results of these investigations and the techniques and instrumentation employed will now be summarized. These descriptions demonstrate the versatility of the shock tube as a facility for conducting hypersonic research better than any broad review of shock tube technology and speculation about its possible applications.

GENERAL DESCRIPTION

The schematic diagram shown in Fig. (1) gives the notation and nomenclature of this paper. The shock tubes used in these experiments have been described in the literature (2), (3), (4), (5). In general, they consist of high pressure drivers depending on combustion of oxygen, hydrogen and helium to create the strong shock waves*. Systematic experiments have shown that especially for large shock tubes the mixing of the combustible gases is extremely important and difficult. If the gases are properly mixed then controlled, non-detonating, complete burning has been found possible for mixtures of oxygen and hydrogen (in stoichiometric ratio) with a diluent helium forming between 70 and 80% of the total mass of the mixture. The strongest shock waves which can be created by combustion of oxygen and hydrogen are produced by mixtures containing 60% helium, which burn quite violently with unpredictable detonations. Not much shock strength is lost by diluting the mixture to 70% helium.

The performance of constant volume combustion drivers is quite predictable. The speed of sound in the hot driver gas has been measured from the time interval between the passage of the expansion wave at two pressure gages in the driver. The measurement is in good agreement with sound speeds calculated considering dissociation of water vapor in the combustion products.

The resultant shock strengths attainable are shown in Fig. (2). The experimentally achieved velocities agree reasonably with the calculated predictions. However, this is not a particularly important feature because in general the shock Mach number is not a critical variable as it is usually not required precisely. Reproducibility of a half a Mach number is average for experiments where no special emphasis has been placed on controlling this scatter.

The speed of the shock wave is monitored as it travels down the tube. This measurement has been accomplished in a number of ways. Shock waves are easily detected by pressure, heat transfer, gas conductivity, density and a number of optical measurements. In

---

* Of the many different methods of creating strong shock waves, such as heated light gases, double diaphragms, detonations, solid explosives and electrical discharge, only controllable combustion appears to be at present at the state of development where it can be used reliably.

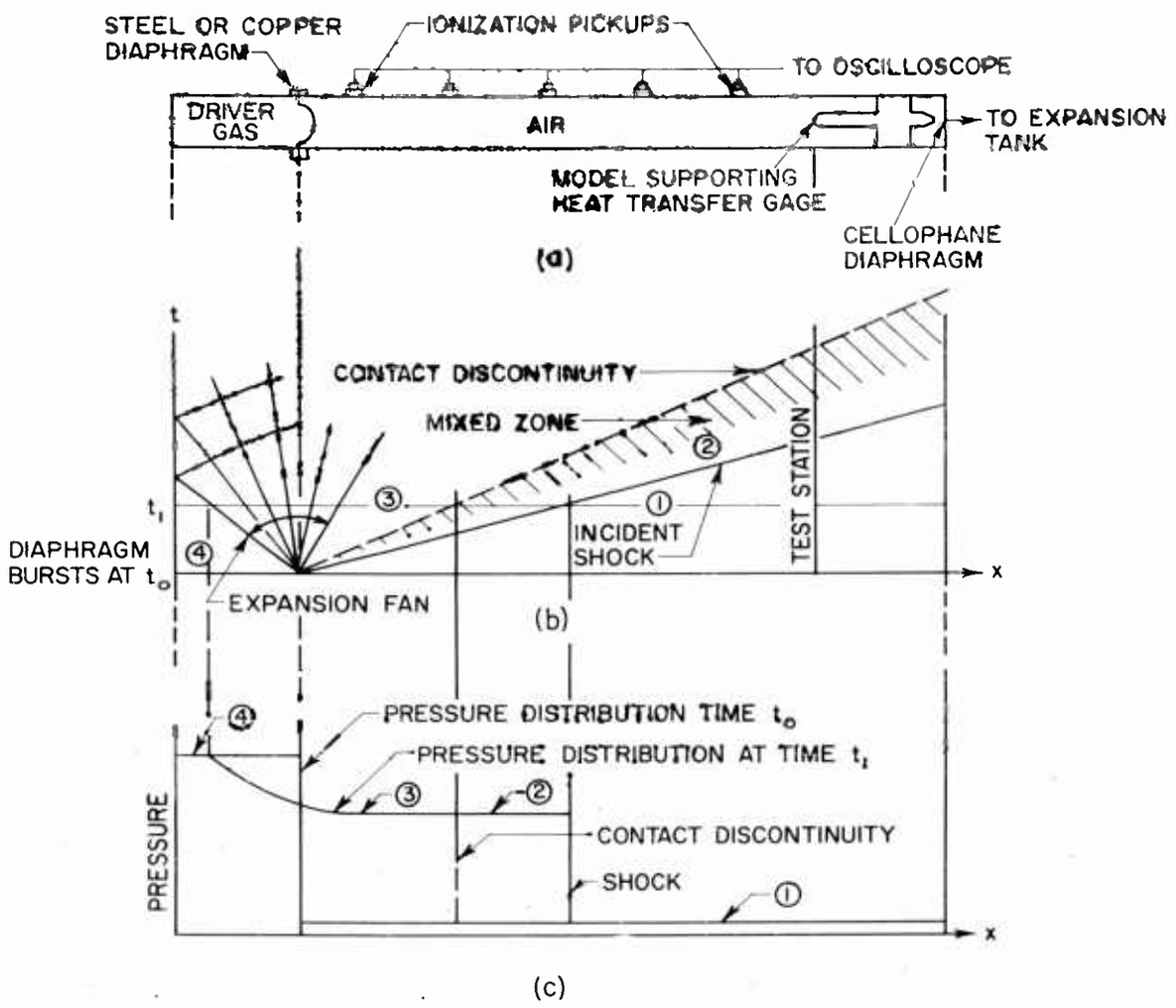

Fig. 1 — (a) Schematic diagram of shock tube.

(b) X-T diagram showing the progress of the shock wave and the expansion wave following the diaphragm burst. The gases which were originally separated by the diaphragm are separated by the contact discontinuity (interface).

(c) Pressure distribution at several typical times in the shock tube. (Time t_o and t_1 from (b)).

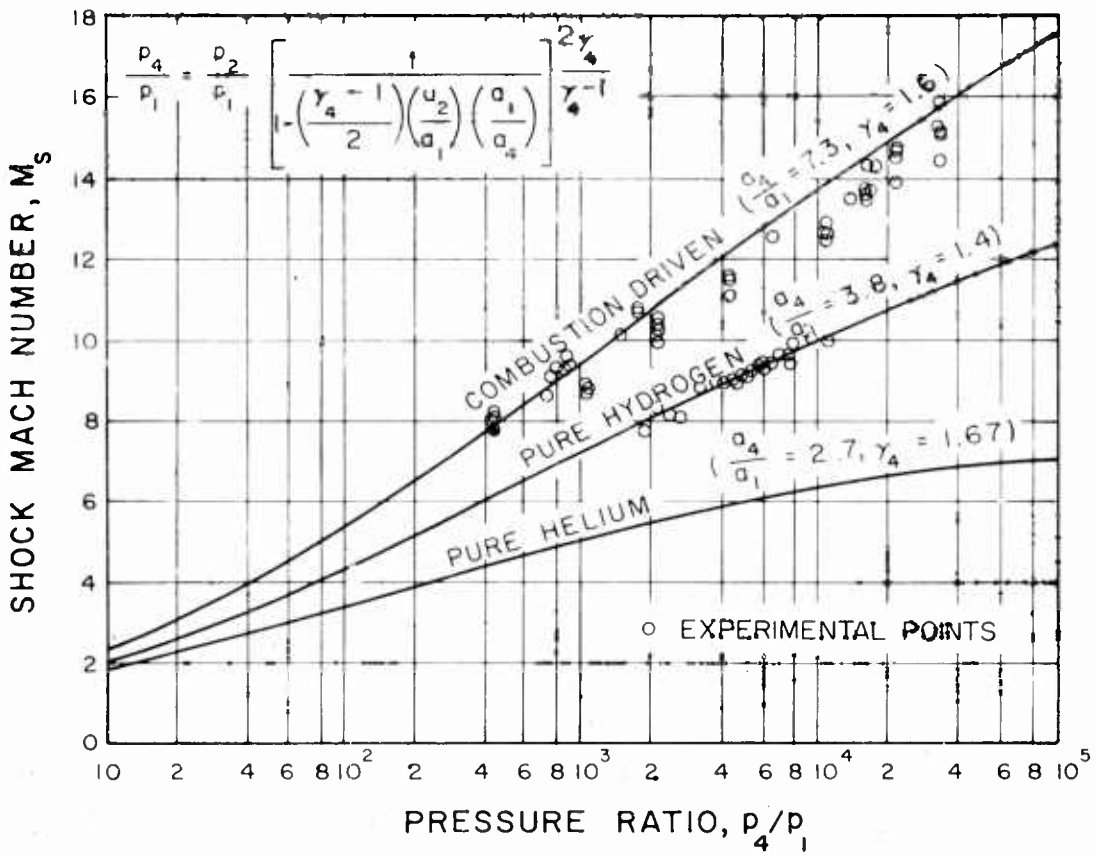

Fig. 2 — Relation between shock Mach number and disphragm pressure ratio for three typical driver gases, (a) combustion of O_2, H_2 and N_2, (b) cold hydrogen, and (c) cold helium (Equilibrium air is the driven gas). Experimentally measured values are shown.

air, in the range of shock wave speeds 8 to 16 times the speed of sound at room temperature, the ionization-sensitive pickup which measures the change of resistance of an air gap, is simple and extremely useful. Almost any degree of accuracy can be achieved by properly choosing the time resolution and pickup spacing. A typical oscillograph is shown in Fig. (3). The sweep of a normal oscilloscope has been extended as a raster so that very long times, resolvable to very small intervals, are displayed. Besides ionization-sensitive pickups, both heat transfer gages and phototubes have been used to measure the shock velocity in the experiments described.

In order to perform experiments in air free of impurities, it has been found advisable to flow gas through the low pressure shock tube section, instead of using a static test gas. This procedure is especially important in spectroscopic work. It has been found that a large amount of extraneous material can diffuse out of the shock tube walls, "o"-rings, etc., if a static, low pressure gas is used. A typical flow system consists of a throttling valve and a check valve (which is closed by the pressure behind the shock wave) near the diaphragm in the gas inlet line, and another check valve aft of the station where measurements are made in a line from a vacuum pump. The flow velocity of the test gas is kept insignificantly small compared to the shock wave speed.

The properties behind a normal shock can be calculated from the conservation laws, i.e., the Rankine-Hugoniot equations. For high temperature applications thermodynamic equilibrium properties of the gas, derived from statistical mechanics, must be substituted for the equation of state. For air, Hilsenrath and Beckett[6], Gilmore[28], and Logan and Treanor[29] have calculated the properties of air in thermodynamic equilibrium. These data have been used by Feldman[7] to solve the normal shock and other typical shock tube and hypersonic flight situations.

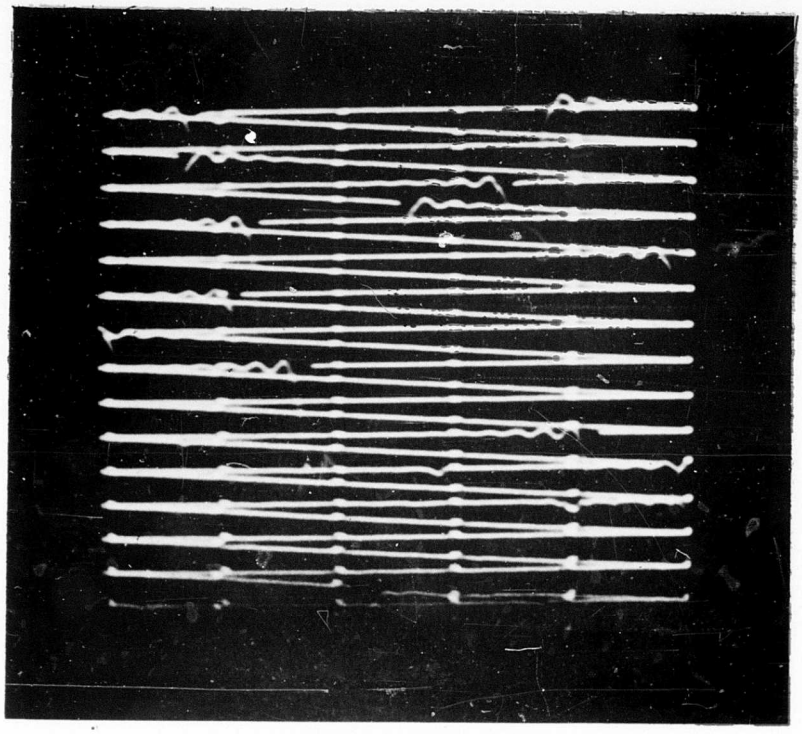

Fig. 3 — Typical oscillograph from the shock velocity timing circuit. The oscilloscope sweep starts at the top and makes a complete cycle, left to right and back, every 100 microseconds. The bright spots are produced by the output from a crystal oscillator, spaced exactly 10 microseconds apart. The time of arrival of the shock wave at each successive ionization-sensitive pickup is denoted by the sudden break in the sweep (change in gap resistance caused by the rapid thermal ionization of the gas). Sample oscillograph has signals from 12 pickups, spaced approximately a foot apart.

THERMODYNAMIC EQUILIBRIUM

Almost all shock tube measurements in high temperature gases by nature of their short steady state depend to some degree on the assumption that thermochemical equilibrium exists in all of the hot gas region. Much research has been pointed at ascertaining this fact. This work has mostly been directed toward measuring vibrational relaxation time or toward studying the dissociation or recombination process. At the lowest temperatures in the region covered by these investigations, $M_s = 6.0$, the vibrational relaxation times in air are already very fast. These rates have been measured by Blackman[26] and others,[23],[24] in oxygen and nitrogen, and are shown in Fig. (4) applied to air under the assumption that the rates applicable are those at the total pressure of the gas, not at the partial pressure of each component. It can be seen that using the rates for the component gases, the vibrational relaxation process is fast enough to leave the test gas in equilibrium. The data available for the relaxation time of either the dissociation or recombination process are not as well defined at the present time.

At the AVCO Research Laboratory two different types of measurements have been made to establish the rates involved in the dissociation and recombination process. First, the Mach angles of very weak waves created by very small surface irregularities have been measured by Feldman[9] on schlieren photographs. The Mach number of the flow is a strong function of the gas state. This measurement has been employed in a number of ways. In the original experiments the Mach number in the flow behind the moving normal shock was measured by inserting a flat plate with a sharp leading edge into the flow. The experimental setup and representative schlieren photographs are shown in Fig. (5). Results from this experiment are plotted in Fig. (6). It can be seen that the Mach number predicted from the equilibrium assumption is actually measured within the scatter of the data. The results from this experiment are conclusive but not very quantitative for obtaining rates.

In an attempt to measure the rate constant for recombination of dissociated air precisely, a shock tube experiment was conceived to give a very rapid expansion of a dissociated gas. A two-dimensional Prandtl-Meyer expansion, after a compression on the leading edge of a wedge, was used. In order to gain the maximum change

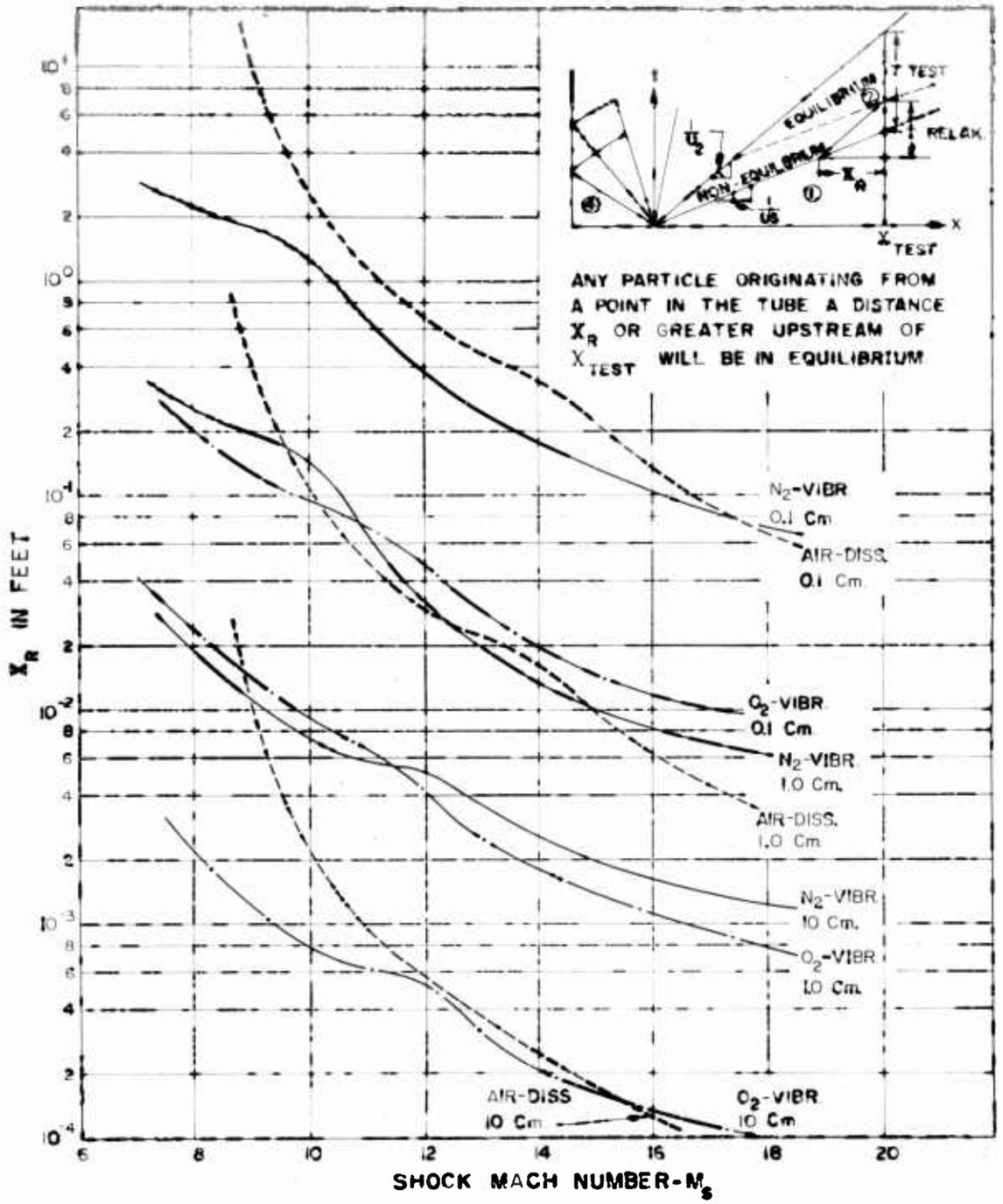

Fig. 4 — Relaxation times behind a moving normal shock wave in a shock tube. The relaxation times (for vibrational relaxation of O_2 and N_2 from Ref. (26) and a dissociative relaxation based on a recombination rate constant, k_r, of 10^{17} cm^6 sec^{-1} mole^{-2} and the equilibrium properties of air [6]) are given in terms of the length of shock tube required for a particle to be immersed in the hot flow, region 2 in Fig. (1), for a length of time equal to the relaxation time.

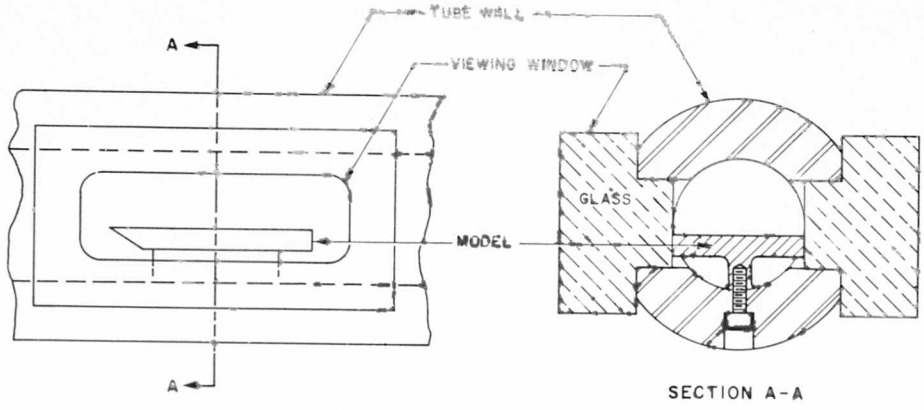

(a)

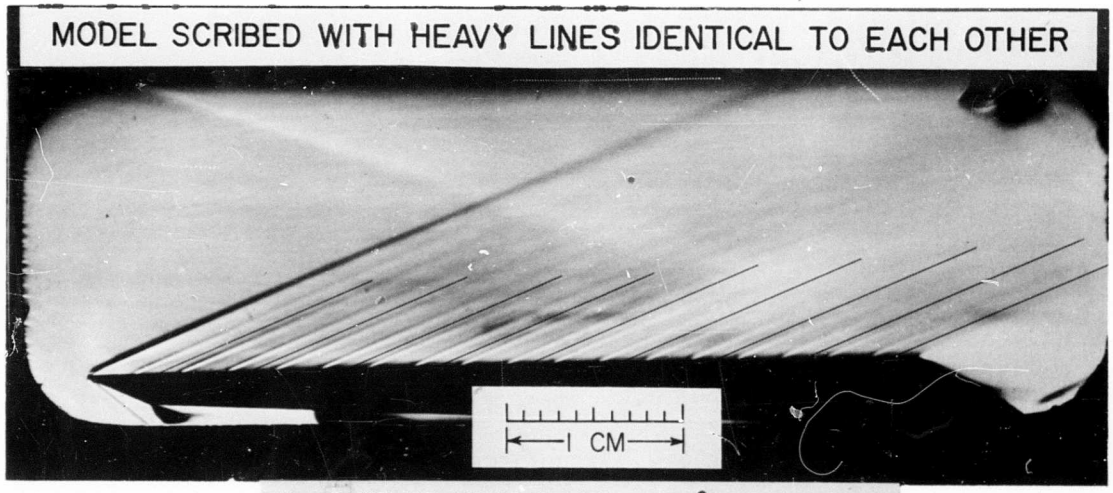

(b)

Fig. 5 — (a) Experimental arrangement of model in schlieren test section in shock tube chemical kinetic experiments.

(b) Schlieren photograph of flow over model showing Mach lines and direction of lines predicted from equilibrium assumption.

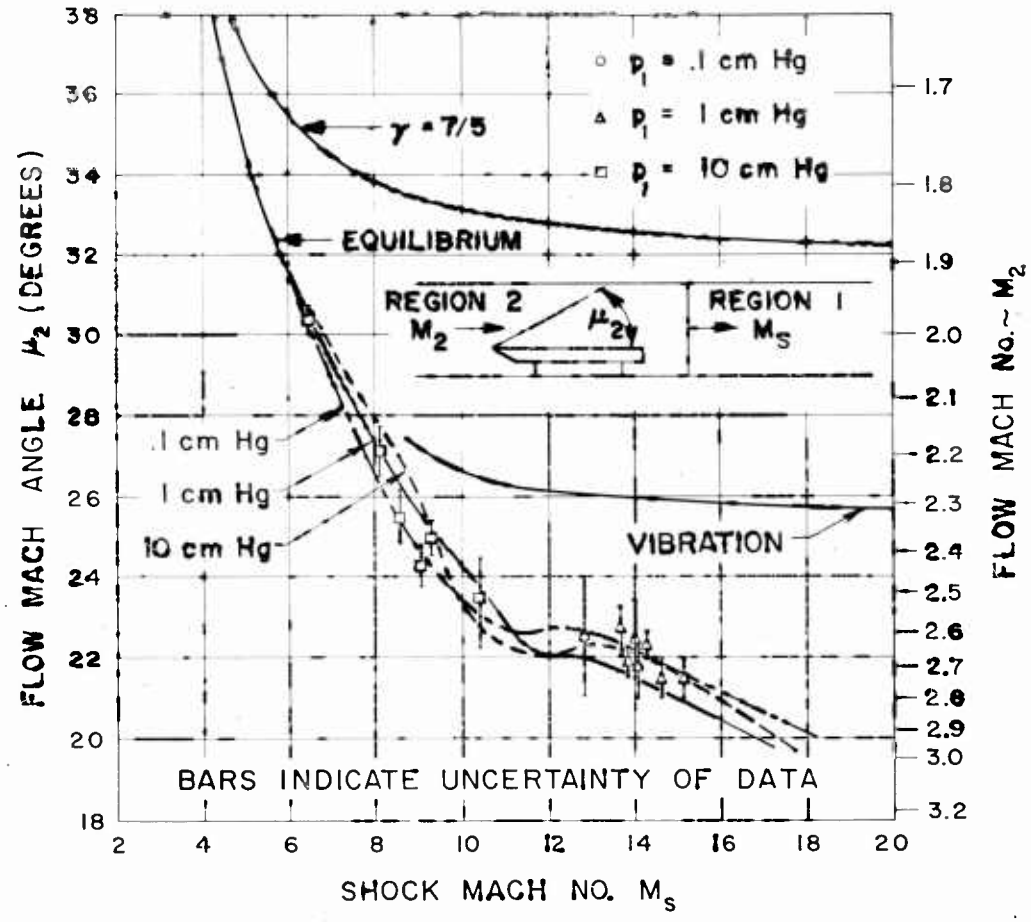

Fig. 6 — Estimates of flow Mach number downstream of moving shock. (Relaxation phenomena are included when computing sound velocities). Comparison of experiments with frozen flow (γ = 7/5), equilibrium flow, and the Mach number which the flow would have if vibration were in equilibrium but no dissociation had occurred.

of Mach number between the extreme chemical processes, i.e., equilibrium and "frozen"* flow, the wedge angle was adjusted to give very nearly sonic flow on its forward edge. Various turning angles of the expansion were used. The general concept of the experiment is that if recombination of atoms takes a long enough time, then small disturbances aft of the corner will create Mach waves which index the local state of the gas. Unfortunately, all measurements of the Mach angle, even from the first disturbance behind the corner, have agreed with values which are predicted from the equilibrium assumption, as shown in Fig. (7). As a result, a rough estimate of a lower limit for the recombination rate constant is the only information that has been obtained from this experiment to date.

As a by-product of this experiment it was observed that the oblique shocks on the forward portion of the wedge assumed an angle predictable from equilibrium theory. This condition is very nearly the same as at the stagnation point of a blunt body. The comparison of the observed and calculated oblique shock angles are shown on Table (1). Details of this work have been reported in Ref. (9).

The second method used by Camm and Keck[25] to observe the rate processes is a system which monitors the radiative relaxation behind a moving normal shock. The radiation behind a moving normal shock is observed through a vertical slit collimated to produce time resolution better than 0.5 μ sec., when the signal is observed by a photomultiplier. The radiation has also been dispersed by a monochromator and viewed over several limited wave length bands.

Results have been obtained in oxygen and nitrogen. The recombination rate constant, kr, at or near equilibrium, obtained from these experiments appears to be in general agreement with the results of Glick and Wurster[24]. A typical oscillograph showing the radiation relaxation is presented in Fig. (8). The rate constant, kr, (in cm^6 $sec.^{-1}$ $moles^{-2}$) estimated to be of the order of 10^{16} for the component gases and essentially independent of temperature by several investigators, appears to be approximately as estimated.

---

* The "frozen" and "equilibrium" situation can best be distinguished by considering the relaxation time for recombination of atoms τ_R as compared to a characteristic flow time, τ_F. The frozen flow is defined as $\tau_R \gg \tau_F$ and equilibrium as $\tau_F \gg \tau_R$.

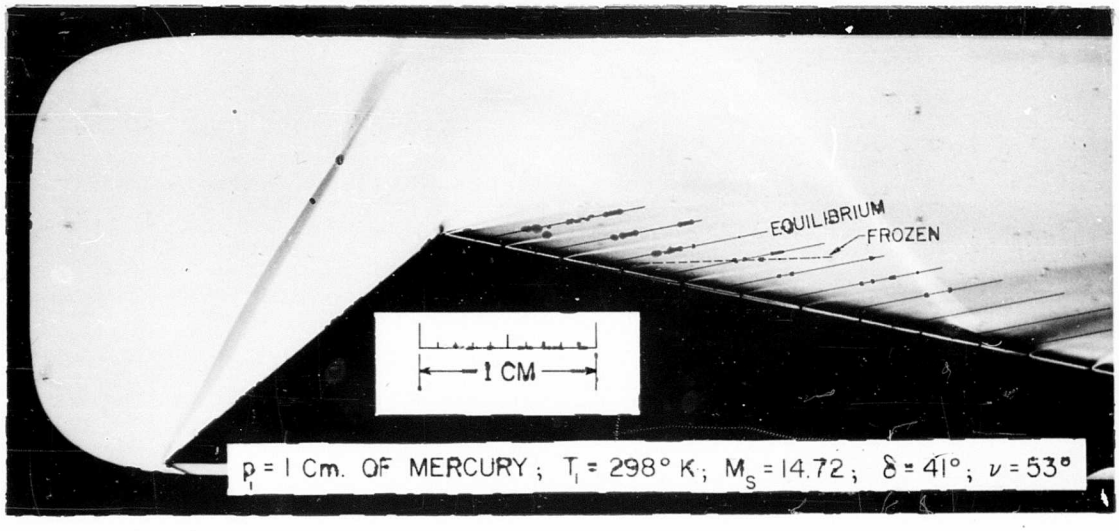

Fig. 7 — Comparison of experimental Mach lines with equilibrium and frozen Mach angles. (M_{equil} = 2.56, μ_{equil} = 23.0°).

TABLE I — OBLIQUE SHOCK EXPERIMENTS

Run	p_1 cm. Hg.	M_s	δ	β_{exp}	β_{ee}	β_{ef}	$\beta_{exp}-\beta_{ee}$	$\beta_{exp}-\beta_{ef}$
				exp	ee	ef		
F-145	0.1	15.6	26.0	39.5	39.5	48.1	0.0	-8.6
F-146	0.1	16.0	26.0	39.0	39.2	47.9	-0.2	-8.9
F-70	0.1	14.75	27.0	41.0	41.0	50.2	0.0	-9.2
F-141	0.1	14.15	33.0	49.0	49.6	D	-0.6	—
F-74	0.1	12.57	41.0	63.0	63.0	D	0.0	—
F-50	0.1	14.15	43.0	63.7	64.3	D	0.4	—
F-140	0.1	16.90	43.0	59.6	59.4	D	0.2	—
F-232	1	13.15	20.0	37.5	37.5	40.1	0.0	-2.6
F-142	1	13.35	25.0	41.5	41.9	46.6	-0.4	-5.1
F-143	1	14.60	25.0	40.7	40.7	45.8	0.0	-5.1
F-47	1	13.85	25.7	41.8	42.1	47.3	-0.3	-5.5
F-129	1	13.65	26.0	43.0	42.4	47.8	0.6	-4.8
F-130	1	14.40	26.0	41.5	41.9	47.4	-0.4	-5.9
F-131	1	14.65	26.0	42.0	41.7	47.2	0.3	-5.2
F-133	1	15.15	26.0	40.7	41.2	47.0	-0.5	-6.3
F-76	1	13.65	26.7	43.3	43.2	48.9	0.1	-5.6
F-8	1	14.10	28.8	45.6	45.0	52.1	0.6	-6.5
F-53	1	14.85	33.0	50.8	49.4	63.7	1.4	-12.9
F-56	1	15.25	36.3	54.0	53.5	D	0.5	—
F-20	1	14.40	37.0	55.3	55.7	D	-0.4	—
F-19	1	15.30	37.0	54.8	54.5	D	0.3	—
F-25	1	14.91	38.0	57.0	56.7	D	0.3	—
F-27	1	14.72	41.0	63.7	63.2	D	0.5	—
F-54	1	15.65	43.0	67.0	67.1	D	-0.1	—
F-147	10	9.80	20.8	40.0	40.0	41.7	0.0	-1.7
F-138	10	8.10	26.0	49.8	50.2	58.2	-0.4	-8.4
F-144	10	8.10	30.0	56.0	56.3	D	-0.3	—
F-139	10	8.40	30.0	54.9	55.4	D	-0.5	—
F-137	10	8.80	30.0	53.8	53.8	D	0.0	—
F-136	10	9.80	30.0	52.7	52.3	D	0.4	—

D: detached
δ: deflection angle
β: oblique shock angle

Subscripts

exp : experimental
ee : full equilibrium
ef : equilibrium through incident shock and frozen chemistry, vibration fully excited across oblique shock.

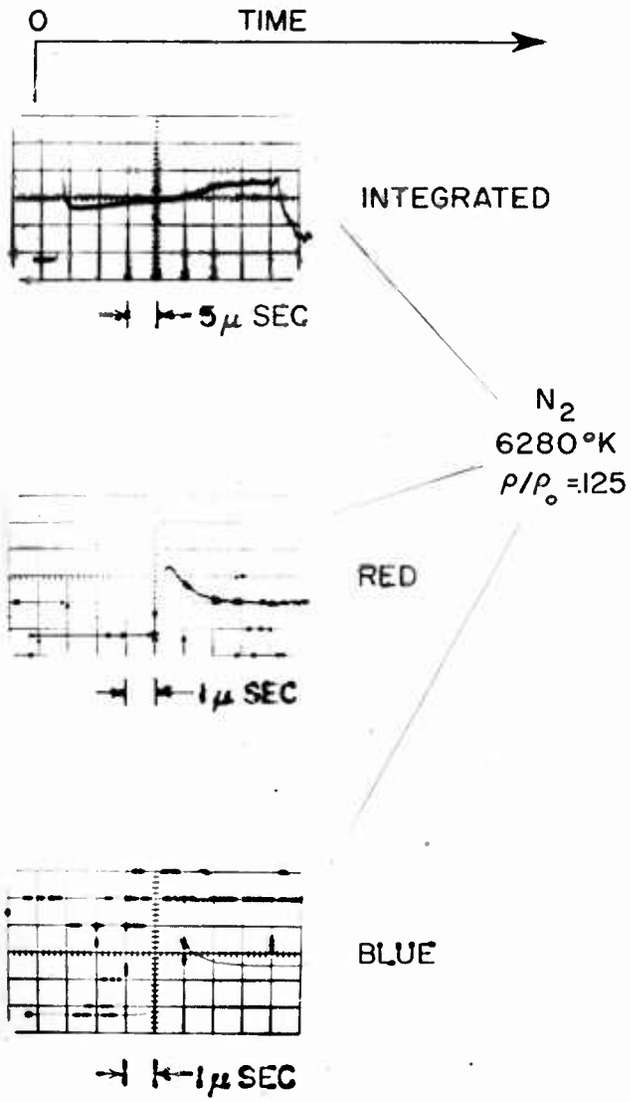

Fig. 8 — Photomultiplier traces from radiative relaxation experiment. The radiation in the red and blue bands indicates the same relaxation time even though one contains CN radiation and the other not. Luminous fronts have previously been attributed to CN radiation in other gases.

The relaxation rates in air are likely to be considerably faster than they are for the component gases, due to the possibility that recombination is not a simple three-body process, but proceeds by intermediate steps. As a result definitive results will not be available until direct measurements have been made in air. Indications* are that the rates are at least a factor of ten better than the 10^{16} measured for the component gases. As a result a recombination rate constant of 10^{17} has been used in a calculation to determine the dissociation relaxation time in the shock tube. The results are shown in Fig. (4) and imply that the gas in the shock tube is in chemical equilibrium.

---

* Some of these indications are, besides the direct experiments described above, heat transfer, electrical conductivity and radiative emissivity measurements, all independent and absolute, which each agree only with theoretical predictions based on the fact that the air behind the moving normal shock is in equilibrium.

HYPERSONIC AERODYNAMICS

The inviscid flow at hypersonic Mach numbers is one problem for which the shock tube is severely limited. Still there are advantages because in the flow about blunt bodies, where essentially all the air which enters the boundary layer went through a strong normal shock, the inviscid flow Mach number does not exceed values around three even at Mach 20. As a result the shock tube boundary layer is never radically different from flight. However, the straight shock tube cannot give exactly correct answers for pressure distribution at the proper flow Mach number or density ratio across the bow shock. Our effort in this field has been limited because other types of facilities, such as ballistic ranges, by the use of optical techniques involving measurement of Mach number distribution from Mach lines, appear to be suited for producing significant results. In the shock tube it will suffice to measure the pressure distribution to define the inviscid flow parameters which exist during experiments.

Boundary layer problems which can be separated from the inviscid flow are particularly suitable for investigation in shock tubes. The first and most serious problem studied was the heat transfer through a laminar boundary layer at the stagnation point of blunt bodies[5], [10]. The stagnation point of a blunt body has several advantages which make it particularly attractive for heat transfer experiments. First, the most severe heating occurs at this point; secondly, direct simulation of the flight conditions is possible; and, thirdly, the problem of conductive, convective, and diffusive (diffusion of atoms as differentiated from molecules) heat transfer has been treated theoretically at the laboratory by Fay and Riddell [10], probably the only example of a boundary layer solution which is capable of including non-equilibrium gas effects.

Considering this problem, it can be shown that the heat transfer rate through a laminar boundary layer at the stagnation point at low speeds, where the product of the density and viscosity, ($\rho\mu$), in the boundary layer does not vary from the free stream to the wall and density varies inversely with temperature[11], can be expressed in a non-dimensional form, by

$$Nu/\sqrt{Re} = \text{const.} = 0.763\,\sigma^{0.4} \qquad (1)$$

where Nu, Re, and σ are the Nusselt, Reynolds, and Prandtl numbers, respectively.

The numerical solution of the equilibrium boundary layer problem treated by Fay and Riddell[10] can be correlated by considering the ratio of $(\rho\mu)_s$ at the edge of the boundary layer to $(\rho\mu)_w$ at the wall, as follows:

$$\frac{Nu}{\sqrt{Re}} = 0.763\,\sigma^{0.4}\left\{\frac{(\rho\mu)_s}{(\rho\mu)_w}\right\}^{0.4}\left\{1 + (L^{0.52} - 1)\frac{h_D}{h_s}\right\} \qquad (2)$$

where L is the Lewis number, and $\frac{h_D}{h_s}$ is the fraction of the total enthalpy which is in dissociation.

From this expression the heat transfer rate, q_s, at the stagnation point can be expressed by

$$q_s = 0.763\left\{(\rho\mu)_w^{0.1}(\rho\mu)_s^{0.4}\left[1 + (L^{0.52} - 1)\frac{h_D}{h_s}\right]\left(\frac{h_s - h_w}{\sigma^{0.6}}\right)\sqrt{\left.\frac{du}{dx}\right|_{x=0}}\right\} \qquad (3)$$

where h_w is the enthalpy of the gas at the wall temperature and $du/dx|_{x=0}$ is the velocity gradient at the stagnation point.

It can be seen from Eq. (3) that simulation of heat transfer requires that the conditions at the edge of the boundary layer are properly reproduced, that the wall conditions be similar, and that the velocity gradient at the stagnation point have the same value in a model test as in the flight situation simulated. In addition, the chemical state of the air in the boundary layer must be considered.

The solutions of the Rankine-Hugoniot equations, Ref. (7) and Fig. (2), make it evident that the stagnation density and enthalpy encountered in hypersonic flight are easily accessible in ordinary shock tubes. In addition, material limits demand that the wall temperatures be similar in the two situations.

The velocity gradient at the stagnation point is derived from

the pressure distribution. In hypersonic aerodynamics the Newtonian estimate has been found to predict the correct pressure distribution very closely even at surprisingly low Mach numbers for blunt bodies. This estimate is independent of the Mach number of the flow. Optical measurements of Mach angles in the flow from schlieren photographs have been used mostly* From the Mach number distribution the pressures can be calculated by following an isentropic expansion on a graphical representation of the equilibrium properties of air, such as the Mollier diagram of Ref. (7). A typical Schlieren photograph and the pressure distribution calculated therefrom are shown in Fig. (10). The pressures are compared to the Newtonian estimate and show reasonable agreement. In particular the pressure near the sonic point is in good agreement. As a result, it is concluded that the velocity gradient at the stagnation point can be taken as the Newtonian value in the shock tube as well as in hypersonic flight and therefore is independent of the Mach number in front of the bow shock.

As a result of these arguments, it is seen that the shock tube can produce the environment encountered at the stagnation point in hypersonic flight. The initial shock tube conditions, and the flight velocity and altitude at which the same stagnation enthalpy and density exists, can be specified. Fig. (11) is a plot of such simulation. The region covered by the stagnation point measurements described is outlined. Trajectories for a number of contemplated hypersonice vehicles have been added to this chart from Ref. (12). The straight shock tube is seen to cover much of the critical heat transfer region.

The considerations outlined so far are complete if the flow chemistry is similar, i.e., if the boundary layer in both the shock tube and flight is either frozen or in equilibrium. In small scale tests, the boundary layer is much thinner than it is on the larger body and an atom therefore spends less time diffusing from the boundary layer edge to the wall. As a result there are situations in which the chemistry is not exactly simulated.

The case where the boundary layer is neither in equilibrium nor completely frozen, but has a finite recombination rate for atoms, has been analyzed by Fay and Riddell [10]. In this reference it is shown that the laminar boundary layer problem can be solved by considering a recombination rate parameter. A constant value of

---

* In our high Mach number shock tubes, the testing time is so small, Fig. (9), that the requirements on a pressure transducer are very severe.

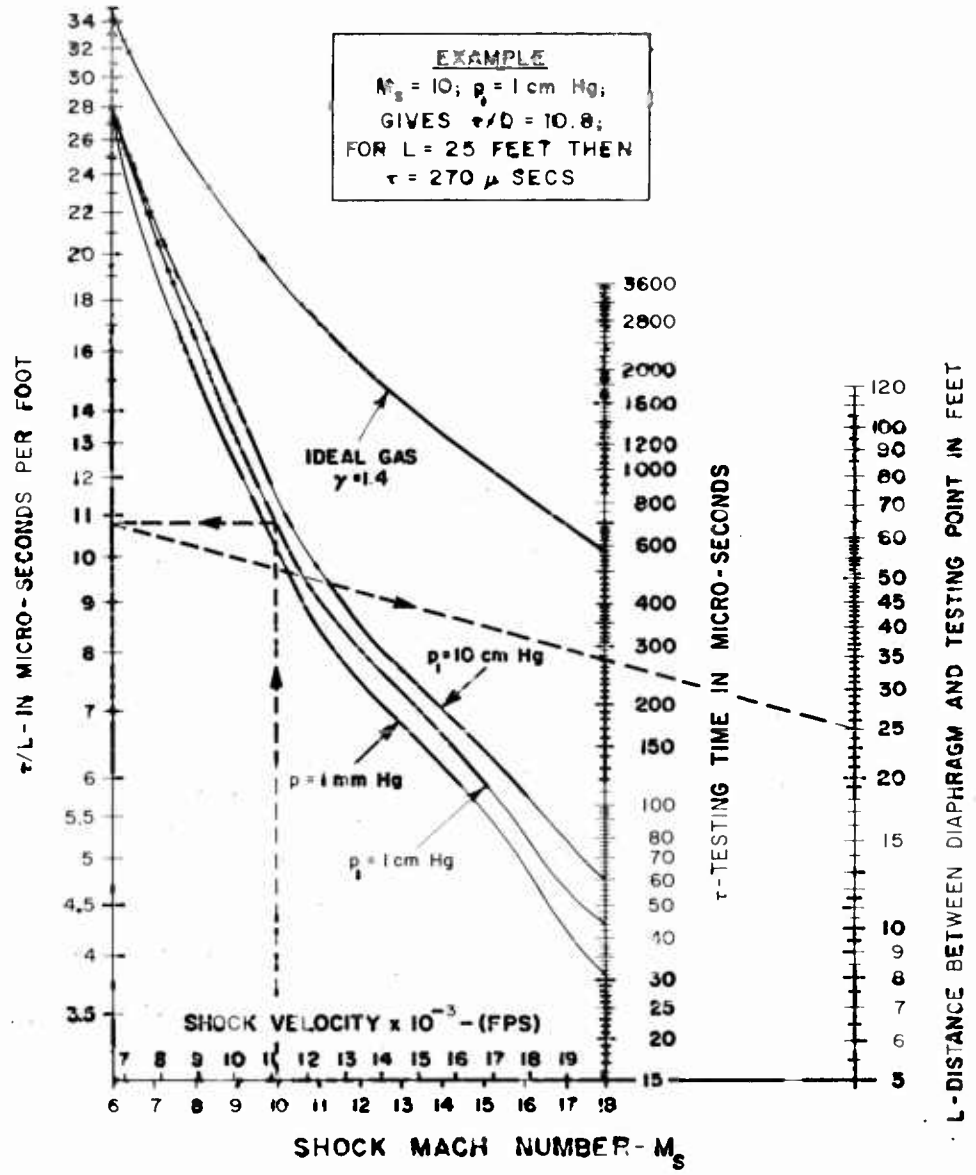

Fig. 9 — Time interval between the arrival of the shock wave and the driver gas at a given station in a shock tube. Calculations have been carried out considering air an ideal gas, (γ = 1.4), and in equilibrium. For equilibrium air the testing time is greatly reduced.

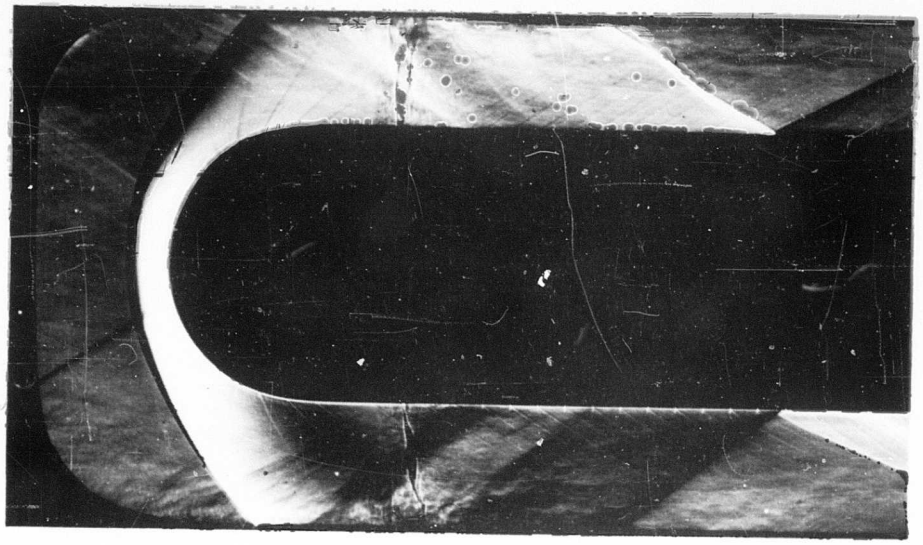

(a)

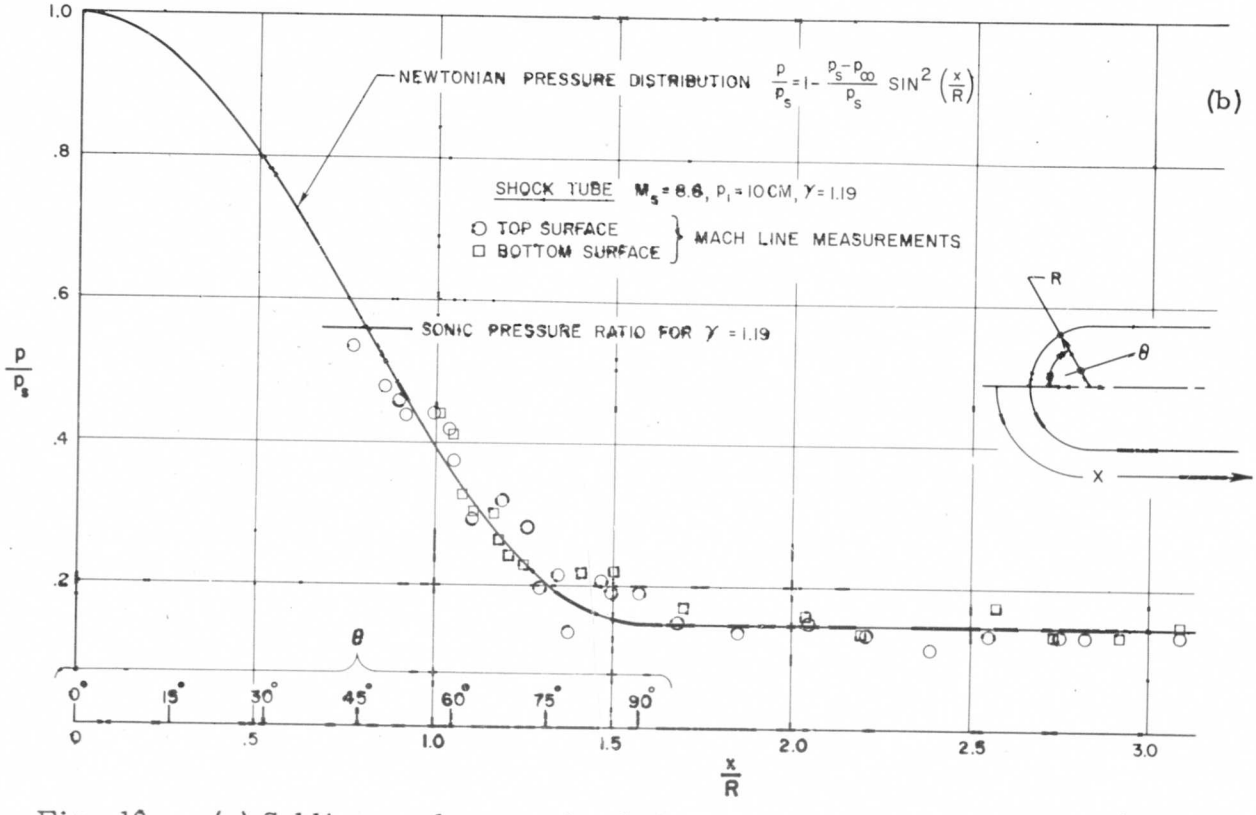

(b)

Fig. 10 — (a) Schlieren photograph of the flow over the nose of a hemisphere-cylinder model in a 1-1/2 inch I. D. shock tube. Note fine Mach lines whose inclination to the body is accurately measurable.

(b) Pressure distribution calculated from Mach line measurements compared to the Newtonian pressure distribution. The agreement is reasonable, especially on the aft portion of the body and near the sonic point.

Stagnation conditions are equivalent to a flight velocity of approximately 13,000 ft/sec and an altitude of 25,000 ft. The flow Mach number is approximately 2.3.

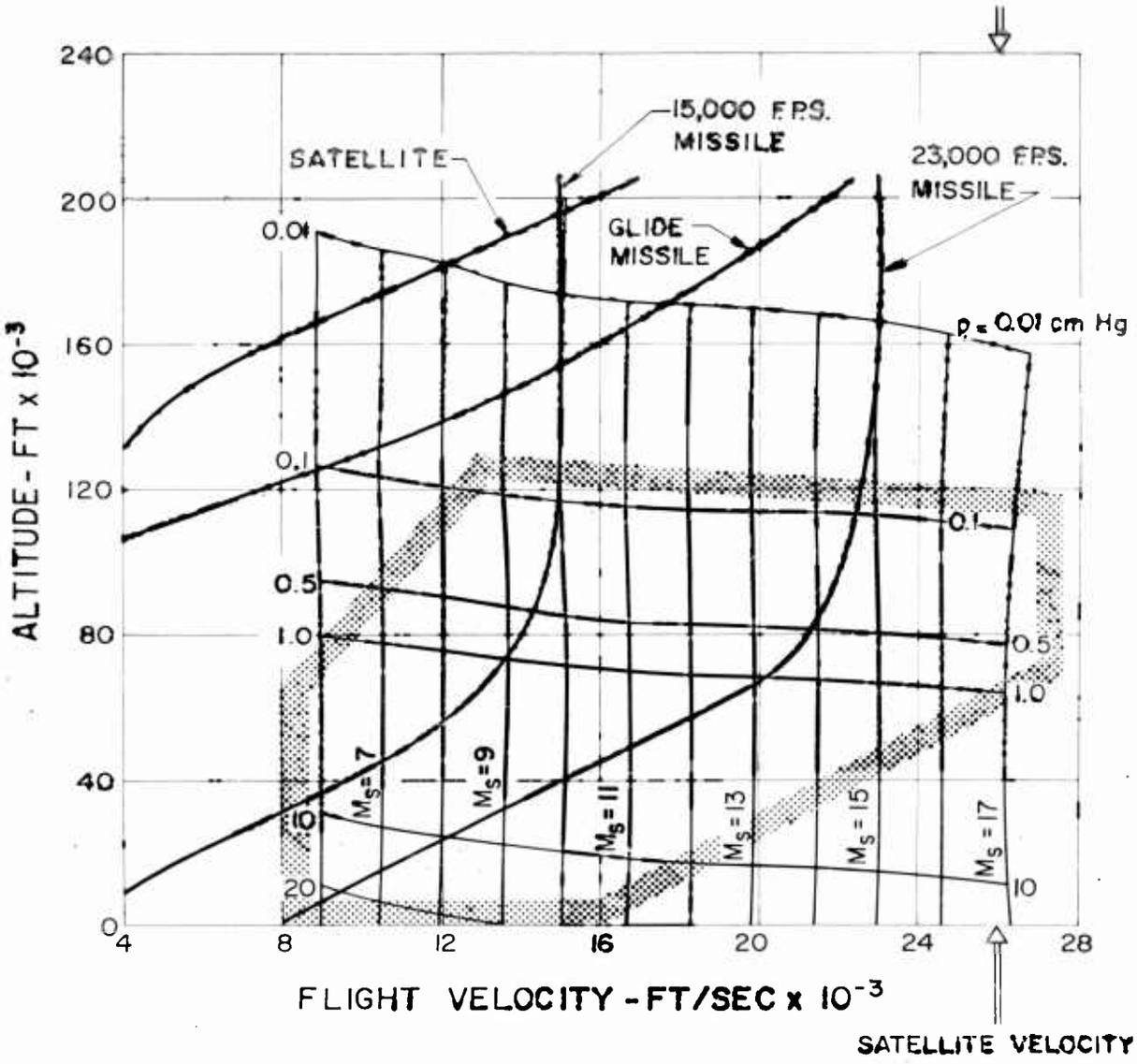

Fig. 11 — Shock tube conditions, M_S and p_1, compared to the flight velocity and altitude at which the same stagnation enthalpy and pressure are encountered. The outlined region is covered by the present experiments.

Typical trajectories of several types of hypersonic vehicles are shown from Ref. (12).

this parameter implies that in addition to the stagnation enthalpy, the flow chemistry in the boundary layer is simulated. At a given flight velocity, and therefore stagnation temperature, the recombination rate parameter is proportional to the square of the density and a model body radius. Experiments performed on a scale model at a given density simulation, actually produce the density which occurs in flight at much higher altitudes, depending on the scaling, even if the boundary layer is not completely in equilibrium. The altitudes at which the chemistry is simulated for a 1/1000 scale model are shown in Fig. 12).

In order to make significant heat transfer measurements, an instrument capable of microsecond response was required. The most promising schemes considered, both variations of the resistance thermometer principle, were (1) surface temperature measurements as used by the Princeton group[26] and others[31], and (2) calorimetric measurements devised and introduced by this laboratory.

From considerations of the one-dimensional heat conduction problem for a finite metal thickness backed by a semi-infinite electrical insulator, the heat flux into the gage for both these schemes can be found.

The two extremes for the ratio of the gage thickness, ℓ, to the characteristic diffusion depth, $\ell_i = k_i\tau$, yield the results for the two types of gages. If the gage thickness, ℓ, is very small compared to ℓ_i in the metal then the gage has essentially no heat capacity and assumes the surface temperature of the insulator[13][31][32]. A constant heat flux, q, gives a voltage, E(t), which is proportional to the instantaneous surface temperature. The shape of E(t) is simply a parabola since the surface temperature rises with the square root of time.

$$q = \text{const.}\ \frac{E(t)}{\sqrt{t}} \qquad (4)$$

In the other extreme, where the thickness, ℓ, is much larger than the characteristic diffusion depth, the temperature at $x = \ell$ is not affected during a test so that no heat is transferred from $x = \ell - \Delta x$ to $x = \ell$. In this case the total heat input must be reflected in the average temperature rise and the heat capacity of the gage. The gage integrates the total heat input, therefore, the

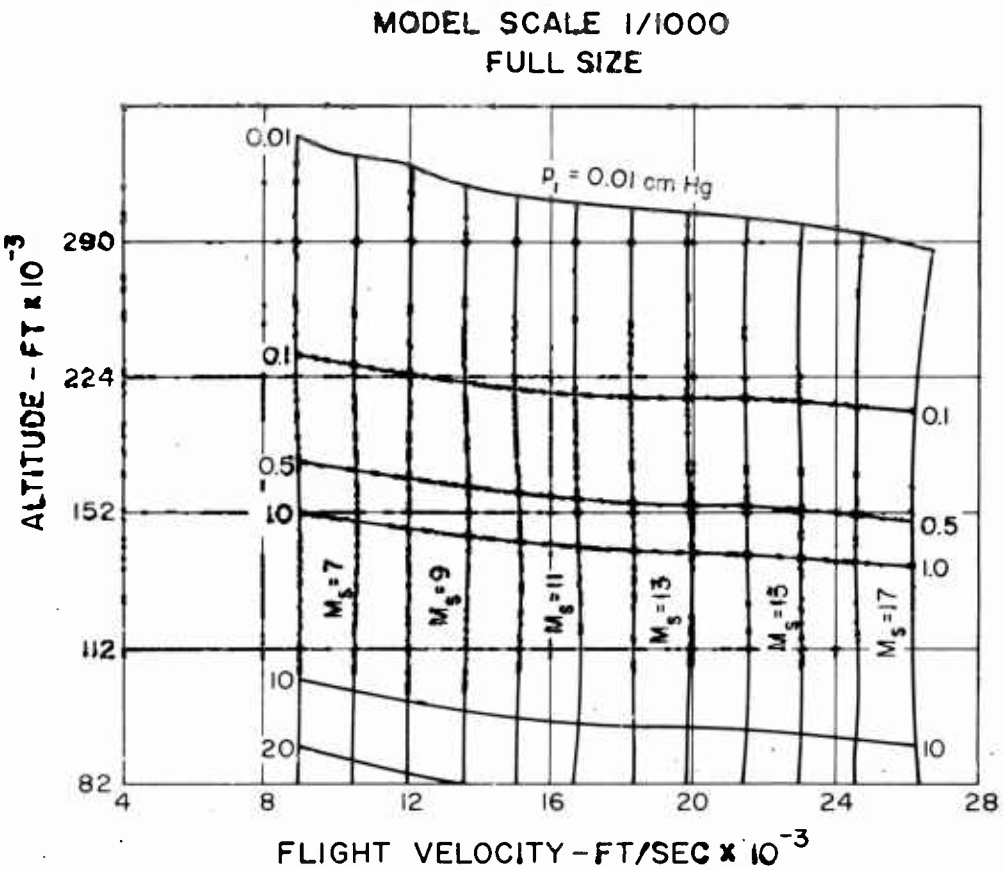

Fig. 12 — Shock tube M_s and p_1 compared to the hypersonic flight condition at which the stagnation point enthalpy and flow chemistry are identical for a model scale of 1/1000.

voltage output varies directly proportional to the total heat input. The instantaneous heat flux is determined from:

$$q = \text{const.} \frac{dE}{dt} \tag{5}$$

Both the above analyses can be extended to the case where the heat flux varies with time, i.e., $q = q(t)$.

Each type of gage has limitations which must be considered. The thin gage cannot be so thick that it has significant heat capacity and causes surface temperatures noticeably different from the one-dimensional semi-infinite case. The thick gage in turn must be thick enough so that the heat loss from the rear of the gage is small. The detailed analysis and investigations made to evaluate the two heat transfer gage principles are given in Ref. (13).

The advantages of the calorimeter gage are that much higher total heat inputs can be handled without creating excessive surface temperatures and that the data reduction, especially for time dependent heat transfer rates, is much simpler. In addition, the calorimeter gage requires no calibration because the bulk properties of chemically pure metals, such as platinum, are well-known. For the thin gage a calibration technique in which a known electrical energy pulse of the same time duration and energy content is used to determine the constant in Eq. (4).

Both types of gages have been made as simple as possible because at the stagnation point of blunt bodies very strong shock waves produce severe erosion, and destroy the surface and gage element. However, the damage occurs only after the contact surface has passed, as seen from the smooth variation of resistance with time, for both the thin and the calorimeter gages. Typical oscillographs for both types of heat transfer gages are shown in Fig. (13).

The results of the stagnation point heat transfer experiment are shown in Fig. (14). The experiment was conducted at three convenient initial pressures in the low pressure section, p_1 = 10, 1.0, and 0.1 cm of Hg., corresponding to flight altitudes of approximately 20,000, 75,000, and 120,000 feet. The velocity range covered by these experiments extends from velocities at which essentially no dissociation occurs to velocities beyond the satellite speed, about 26,000 ft/sec., where more than 60% of the energy is invested in

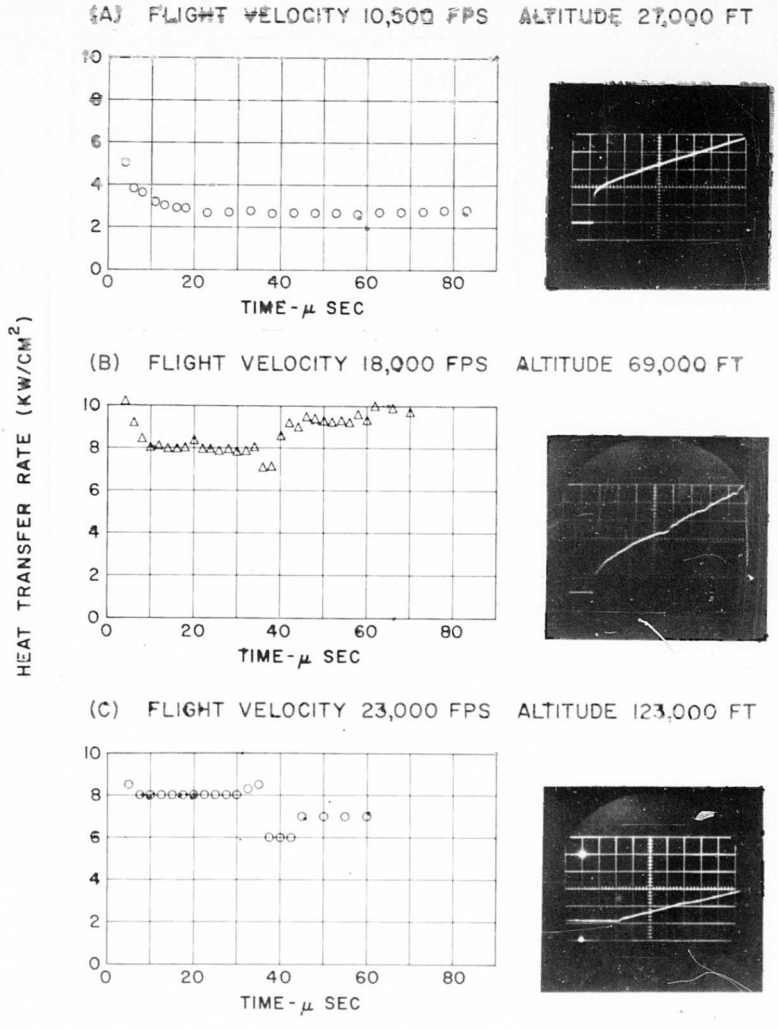

Fig. 13 — Typical oscillographs and data.

On all three oscillographs time increases from left to right. The sweep speed is 10 μ sec/interval. The oscilloscope is triggered before the moving shock arrives at the stagnation point. The break in the horizontal trace denotes the arrival of the shock at the gage. The break of the curve accompanied by the end of the constant heat transfer denotes the arrival of the interface.

(a) Record from a thin heat transfer gage at a relatively low shock Mach number (Note parabolic signal rise)
(b) Record from a thin heat transfer gage at a higher shock Mach number. Note that the extreme conditions at the high stagnation enthalpy degrade the quality of the signal.
(c) Calorimeter gage record. (Note linear signal rise).

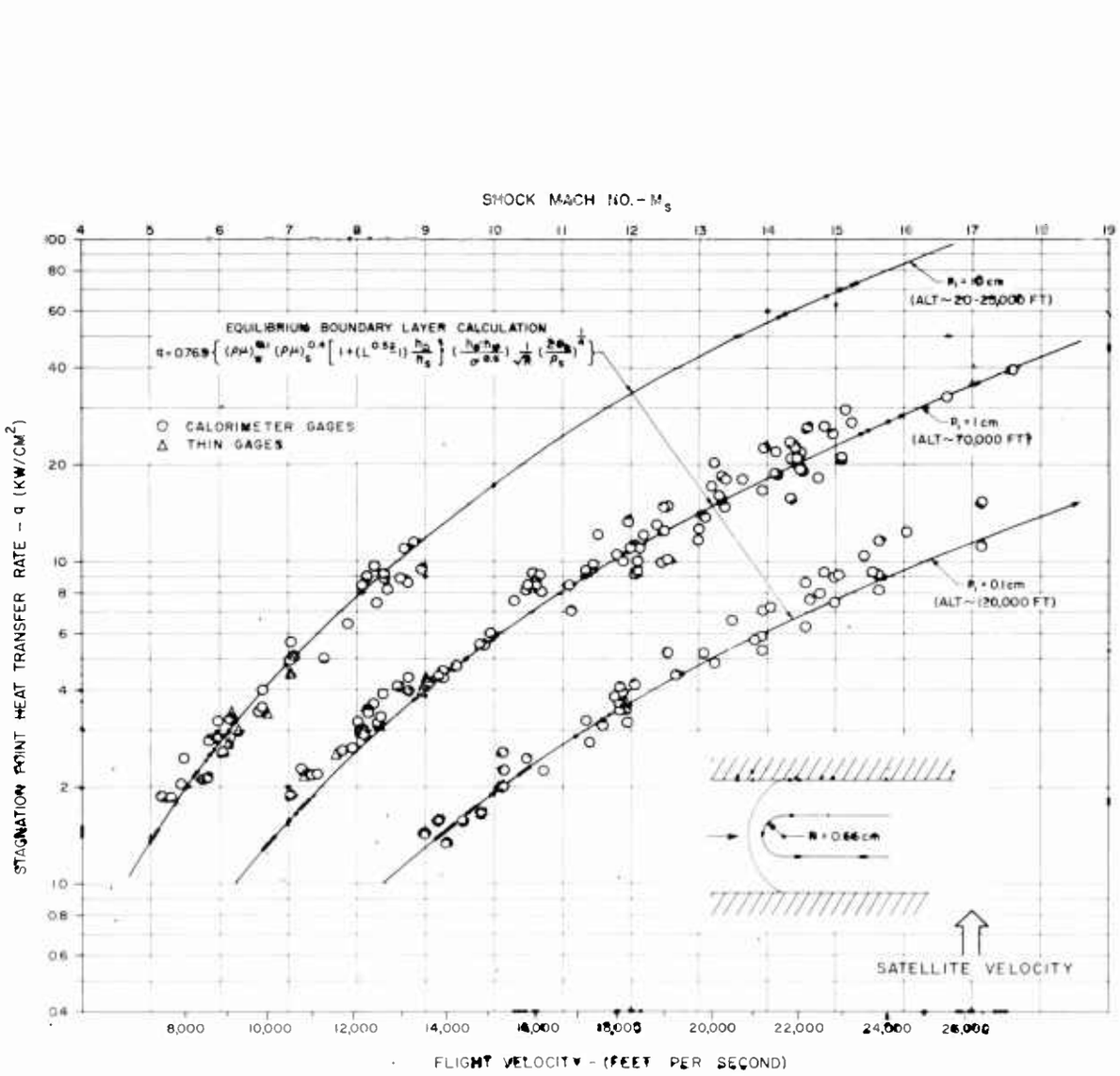

Fig. 14 — **Measured stagnation point heat transfer rates compared to the equilibrium boundary layer theory of Fay and Riddell[10], Eq. (3).**

dissociation energy at the stagnation point. The theoretical curves are plotted from the equation which correlates the equilibrium boundary layer solutions of Fay and Riddell [10], Eq. (3). The Lewis number has been estimated and taken to be 1.4 and the Prandtl number 0.71. The theory and data can be seen to agree within the scatter of the data. An uncertainty in the absolute value of the theoretical prediction, due to the uncertainties in predicting the viscosity and Lewis number of the hot gas, is of the same order as the scatter of the data.

As discussed previously the significance of this data can be extended to higher altitudes if simulation of the boundary layer chemistry, based on the recombination parameter is considered. The best available estimates of the recombination rate, such as the data of Ref. (9) and (23), introduced into the non-equilibrium boundary layer solution of Fay and Riddell [10], indicate that the boundary layer is neither in equilibrium nor completely frozen for the experiments performed at initial pressures of 0.1 cm of Hg. However, the total heat transfer by conduction and convection is very nearly the same for the frozen and the equilibrium boundary (at Lewis number of 1.4) except in the extreme case where the boundary is completely frozen and the wall is non-catalytic to the atom recombination. Because for present recombination rate estimates, the boundary layer is still only partially frozen at $p_1 = 0.1$ cm., the present experiments are not capable of defining the flow chemistry from heat transfer measurements. These effects are discussed in detail in Ref. (10).

If the air were not to equilibrate across the bow shock at the stagnation point, the stagnation pressure would be reduced and the heat transfer lowered correspondingly. At the extreme of the conditions covered by these experiments, this would amount to a reduction of 20% in the heat transfer rate. However, in view of the evidence presented earlier indicating that equilibrium is attained on the leading edge of a two-dimensional wedge, the gas state is not seriously in doubt. Further, it was shown that thermodynamic equilibrium is reached across a moving shock and therefore equilibration across the bow shock, where even higher temperatures and pressures exist, will be much more rapid.

EMISSIVITY OF HIGH TEMPERATURE AIR

A second major investigation, undertaken by Keck, Kivel and Wentink[14], was the determination of the radiative emissivity of high temperature air. Prior to the performance of these experiments, rough estimates were made by H. Bethe and H. Meyer at AVCO and others elsewhere which indicated that the NO β and γ bands might have a transition probability (f number of the order of 0.1) which would give a considerable amount of radiant heat transfer. In fact, radiative heat transfer was estimated to be roughly of the same order as the aerodynamic stagnation point heat transfer for a one foot nose radius sphere flying at Mach 20 at 100,000 ft. altitude.

Because radiation, for optically thin layers with small emissivities, scales in direct proportion with the thickness of the radiating gas layer, the direct model test technique is not applicable, mainly, because the radiative energy would be extremely low and difficult to detect. It was decided to study the radiation from a layer of gas shock-heated to the temperature, density and thermodynamic state of interest to hypersonic flight problems by reflecting a strong shock wave from the closed end of a shock tube. The extension to flight configurations remains a geometric problem. A quartz window was inserted in the end of the tube for observation. The original measurements were performed by using the "thin" heat transfer gage, as used for aerodynamic heat transfer measurements, behind a quartz window. These experiments established the order of magnitude and temperature dependence of the integrated radiative energy flux.

For identification of the radiating species and quantitative emissivity measurements, time resolved spectrograms and calibrated monochromator-photocell measurements were made. The spectroscopic work was devoted mainly to identification and measurement of relative intensities of the radiating species. Time resolved emission spectra were obtained in order to separate the radiation which occurs after the driver gases (or mixed region) encounters the reflected shock. Time resolution of about 10 μsec. has been used.

The experimental setup is shown in Fig. (15) and a typical spectrum in the region of 2700 to 4000 Å is shown in Fig. (16). The second positive band system of nitrogen and CN are clearly detectable. Especially at wave lengths smaller than 3000 Å the NO band systems are expected to have appreciable intensity [27].

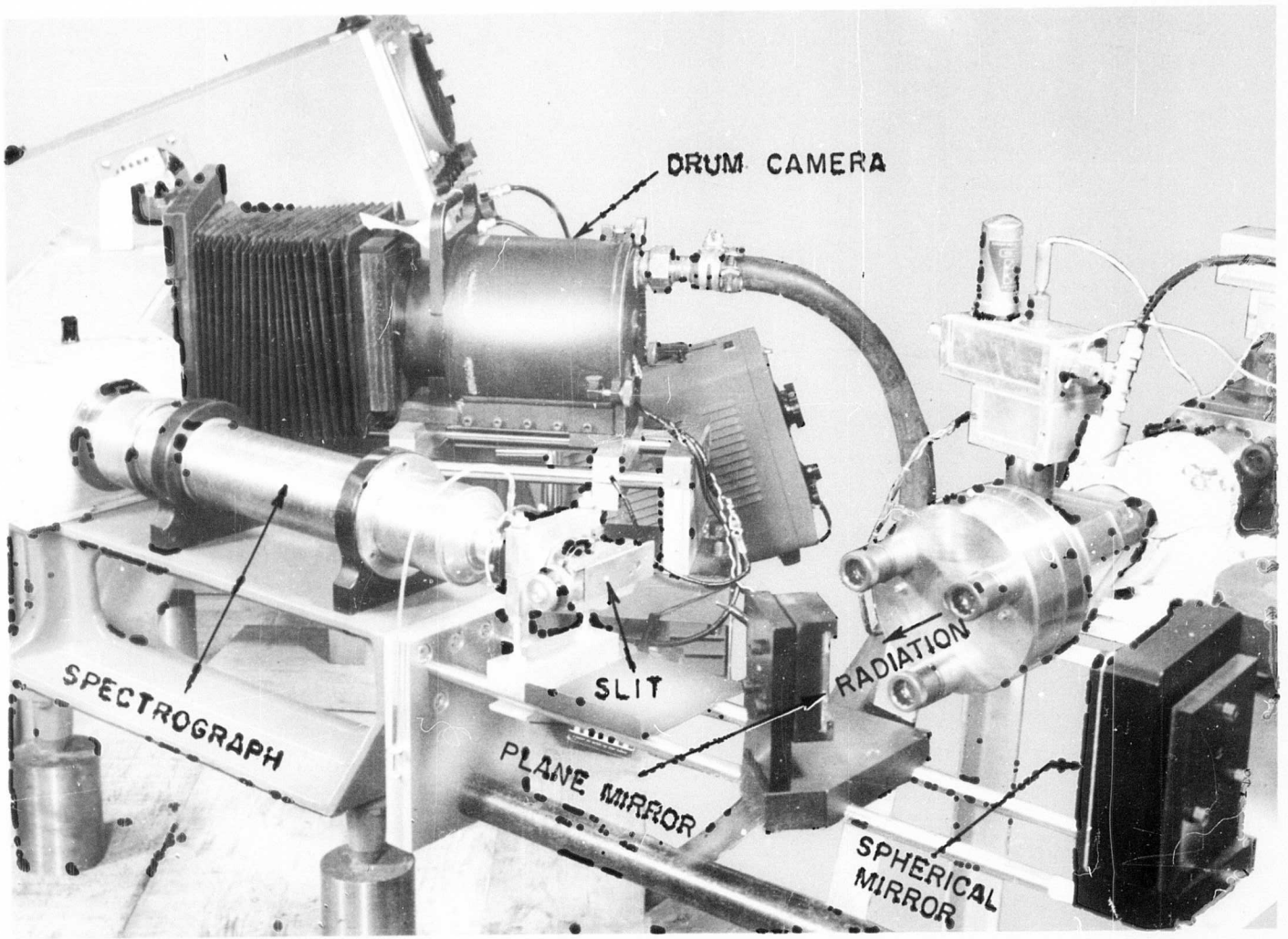

Fig. 15 Experimental arrangement for radiative emissivity measurements, showing end of shock tube, window, spectrograph and drum camera.

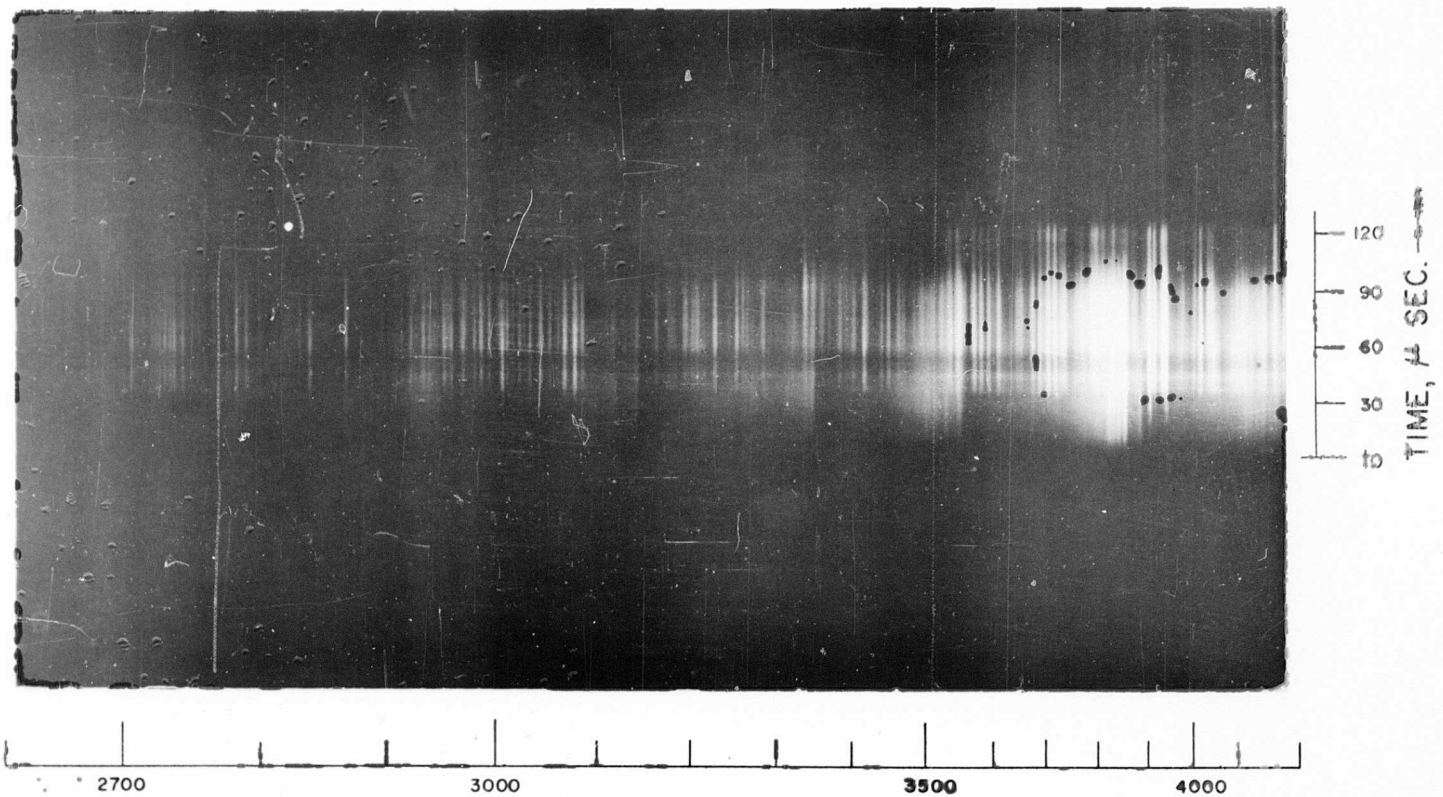

Fig. 16 — Time resolved spectra in the region of 2700 - 4200 Å. Note the build-up of radiative intensity as the gas layer behind the reflected shock grows, and the end of the "clean" radiation at approximately 30 μ sec when the driver gas and reflected shock meet.

Positive identification of NO bands at 8000°K is difficult because of the lack of characteristic structure.

In the visible and near-infrared region, the radiation shows little structure. The radiation above 5500 Å can best be attributed to the First positive system of nitrogen. The CN violet and red band systems are also visible. The lack of structure in the whole region may be due to the reaction of O + electron $\rightarrow O^- + h\nu$, however the continuous distribution makes identification difficult.

Absolute measurements of the spectral emissivity of high temperature air in the region of 2300 Å to 9500 Å have been made, using a calibrated monochromator and photocell. The measurements were made at a shock Mach number of 13.2 ± 0.5 and an initial pressure of 1 cm of Hg., resulting in an equilibrium temperature of 8050°K and a density of ~.85 ± .04 normal atmospheric, sea level density. The measured wave length dependence of radiation from air at a temperature of 8050°K is plotted in Fig. (17). The significant contributing species are tabulated in Table II. where the f numbers and the emissivity of a one cm. thick layer are given. In this table positive spectroscopic identification can be claimed for the CN and N_2 band systems.

TABLE II

Emissivity of optically thin air attributed to six radiating species. The f numbers except for CN are deduced from absolute emissivities at appropriate wave lengths. They are subject to the assumption that the large number of lines in the molecular bands can be treated as a continuum. They are defined as the f numbers per initial electronic state. (Air at ~ 8000°K and ρ/ρ_0 = 0.85)

Source	f number	% emissivity cm^{-1} ϵ/L
NO (β and γ) ($.2\,\mu < \lambda$)	.0025	1.1
N_2 (2 nd. pos.)	.07	1.1
CN (violet)	.1	.1
O^- (free-bound)		.4
N_2 (1st. pos.) ($\lambda < 1\mu$)	.02	.6
O + e (free-free) ($\lambda < 1\mu$)		.1
Total Theoretical Emissivity ($.2 < \lambda < 1\mu$)		3.4
Total Experimental Emissivity ($.2 < \lambda < 1\mu$)		3.5

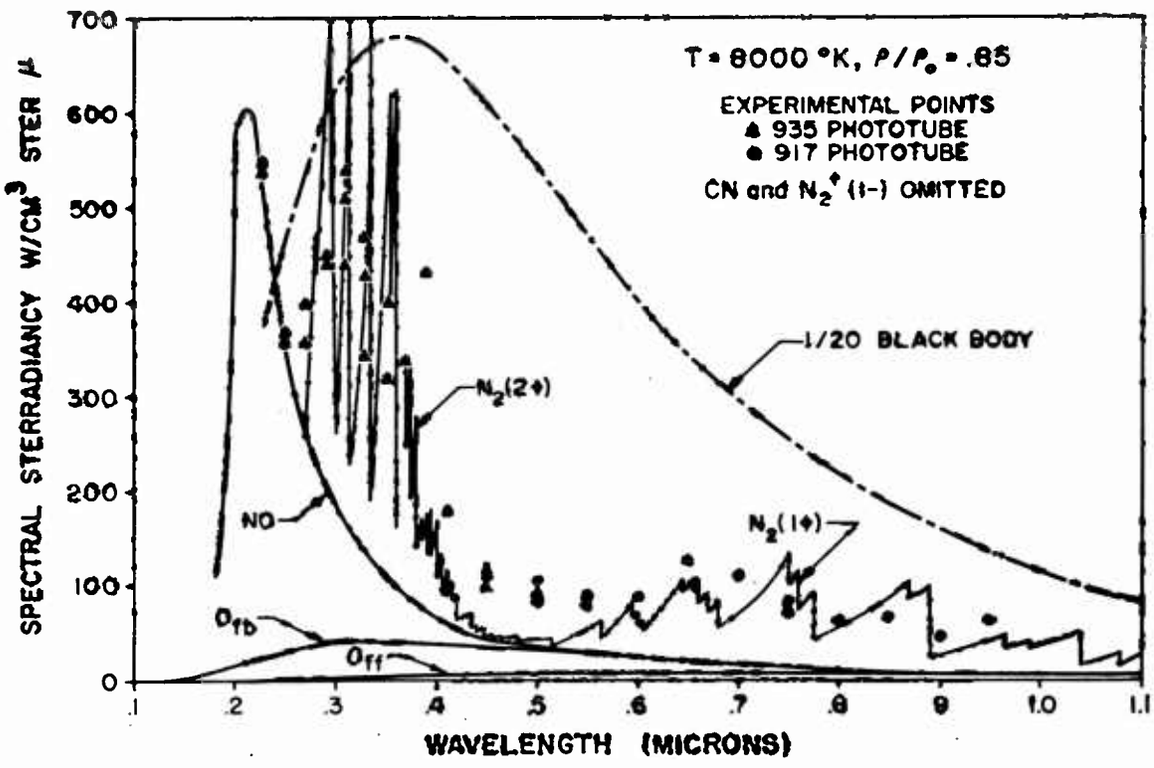

Fig. 17 — Monochromator-photocell measurements of the distribution and absolute intensity of the radiation from 1 cm of air at approximately 8000°K and .85 ρ/ρ_0 compared to the estimated radiation [27].

For the continuum radiation, the theoretical considerations of Kivel[27] coupled with the general features of the spectra make these emissivities plausible*. The theoretical analysis[27], results of which are shown in Fig. (17) together with the measurements, has as free parameters only the f number of the bands of N_2 and NO. These have been adjusted to fit the spectral distributions measured in the appropriate region of the spectrum.

It is important to notice that the f number for NO is considerably less than the estimated 0.1. In addition, the total emissivity is approximately .050/cm. at 8000°K and $\rho/\rho_o = 0.85$. Measurements of the temperature and density dependence of the radiation were made using the monochromator and photocells. The resultant temperature and density dependence of the absolute emissivity per cm. of air is shown in Fig. (18). The results of Fig. (18) can be used to compare the heating at the stagnation point due to radiative heat transfer to the laminar aerodynamic heat transfer rates. It can be shown that in flight at a Mach number of 20 at approximately 120,000 ft., the radiative heat transfer for a one foot radius sphere will be only about 10% of the aerodynamic stagnation point heat transfer.

* The CN and free-free and free-bound radiation associated with oxygen have been estimated based on other data.

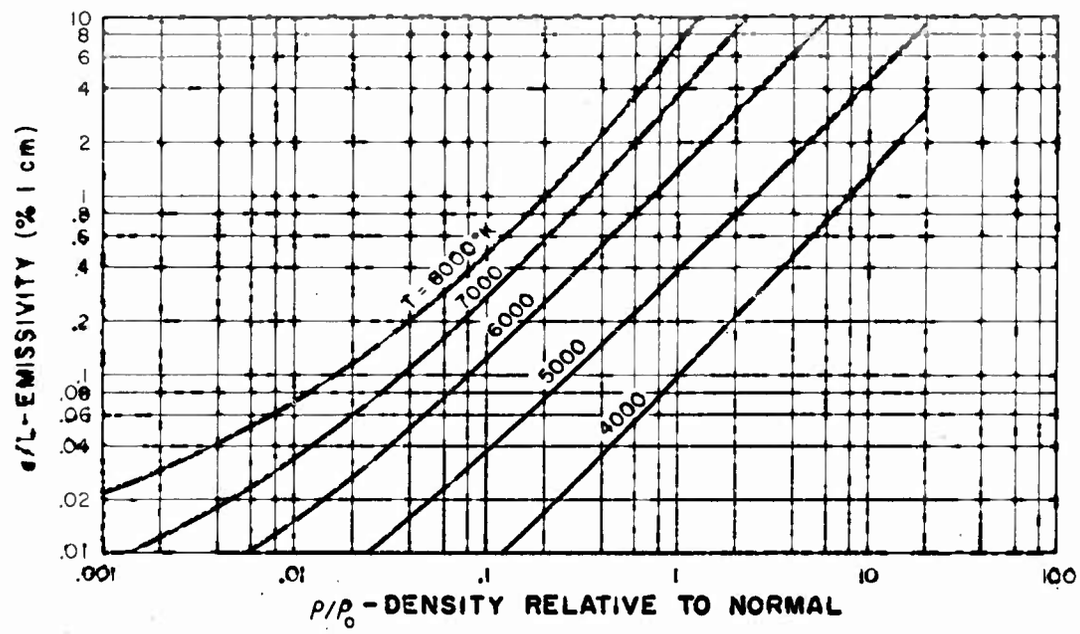

Fig. 18 — Temperature and density dependence of the emissivity of air from the theoretical calculations of Ref. (27). These estimates have been checked in a limited region by the experiments described.

ELECTRICAL CONDUCTIVITY OF HIGH TEMPERATURE AIR

Another investigation carried on at this laboratory is the work of S. C. Lin [15], a study of the electrical conductivity of thermally ionized air.

The techniques employed in this experiment are similar to those reported in detail in Ref. (4). An axisymmetric magnetic field is produced in a glass shock tube section. When the shock heated gas, which is made conducting due to thermal ionization, arrives at, and enters the stationary magnetic field, the magnetic lines of force are displaced. By measuring this displacement of the magnetic field through the use of a small pick-up coil nearby, the electrical conductivity of the gas can be deduced from the known gas velocity and the strength, geometry and displacement of the magnetic field. It is convenient to calibrate the system by shooting a slug of metal of known conductivity through the field at a known speed. A schematic representation of the experimental arrangement is shown in Fig. (19).

Typical oscillogram traces from the pick-up coil signal of this experiment performed at a shock Mach number of 12.0 are shown in Fig. (20), along with the signals obtained in the calibration using an aluminum bar. From the amplitude of the voltage peak and the velocity of both calibration and experiment, and also the known conductivity of aluminum, the gas conductivity can be calculated.

It can be seen from the oscillogram traces that the positive and negative pulses are the same amplitude in the shock tube, as well as for the aluminum bar, which implies that the electrical conductivity distribution must be quite uniform throughout the hot gas region. Furthermore, since the experimental pulse shape, normalized to the same sweep speed as the calibration, is very similar to the aluminum result, the electrical conductivity and hence the degree of ionization must have built up very rapidly behind the shock front. Since the electrical conductivity or degree of ionization behind the shock front built up very sharply at all shock Mach numbers investigated (M_s = 10 to 18), it may be concluded that the equilibrium degree of ionization was reached almost immediately and maintained for all these experiments.

The measured electrical conductivity in practical units (Mhos/cm is plotted in Fig. (21) compared to theoretically calculated conductivities.

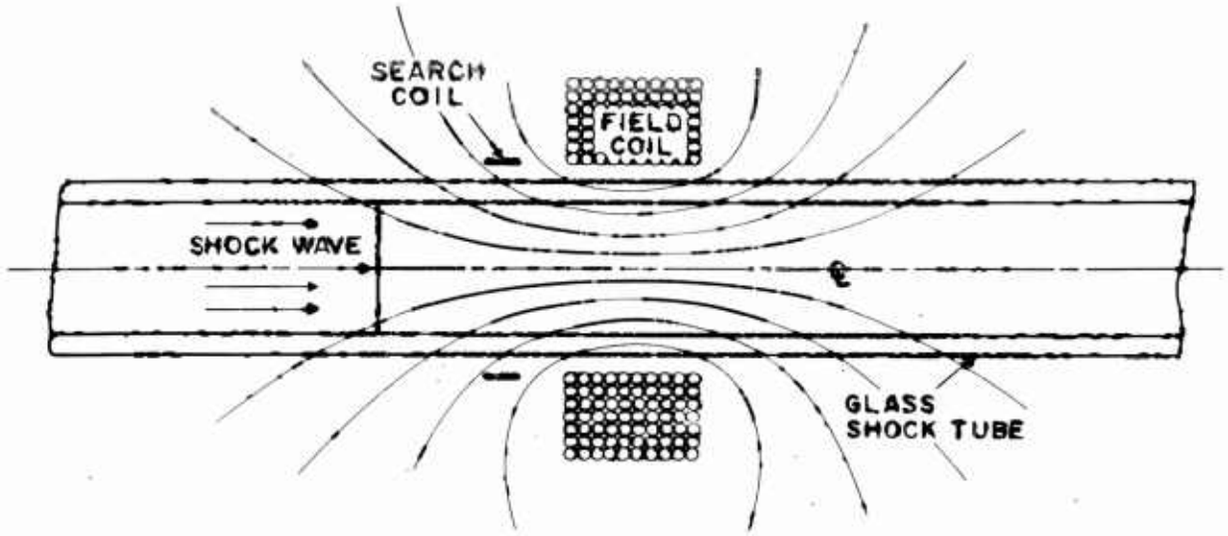

Fig. 19 — **Schematic diagram showing the principal elements of the** shock wave-magnetic field interaction experiment.

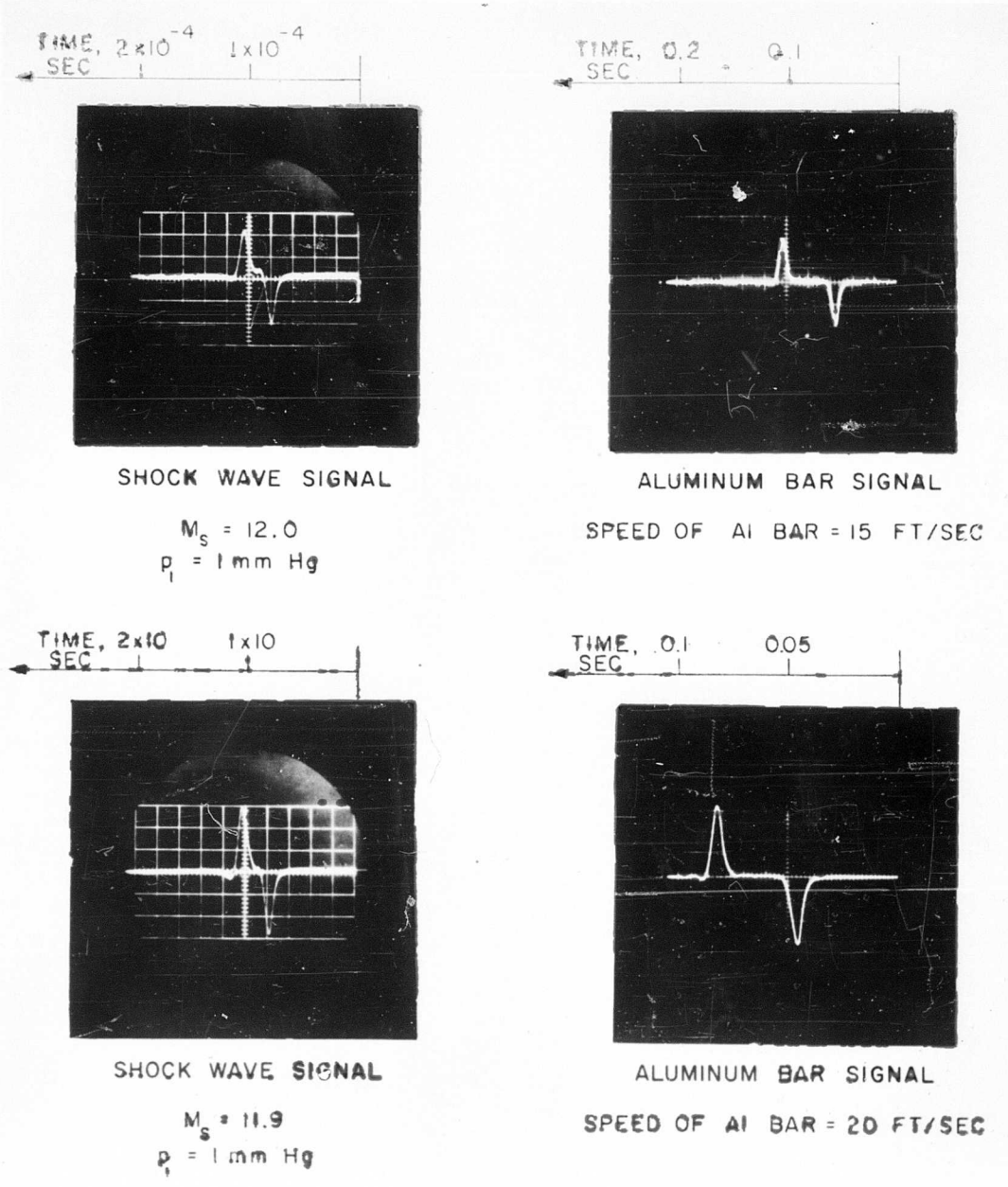

Fig. 20 — Comparison of typical oscillograms from the shock wave and from the aluminum bar calibration in the magnetic field interaction experiment.

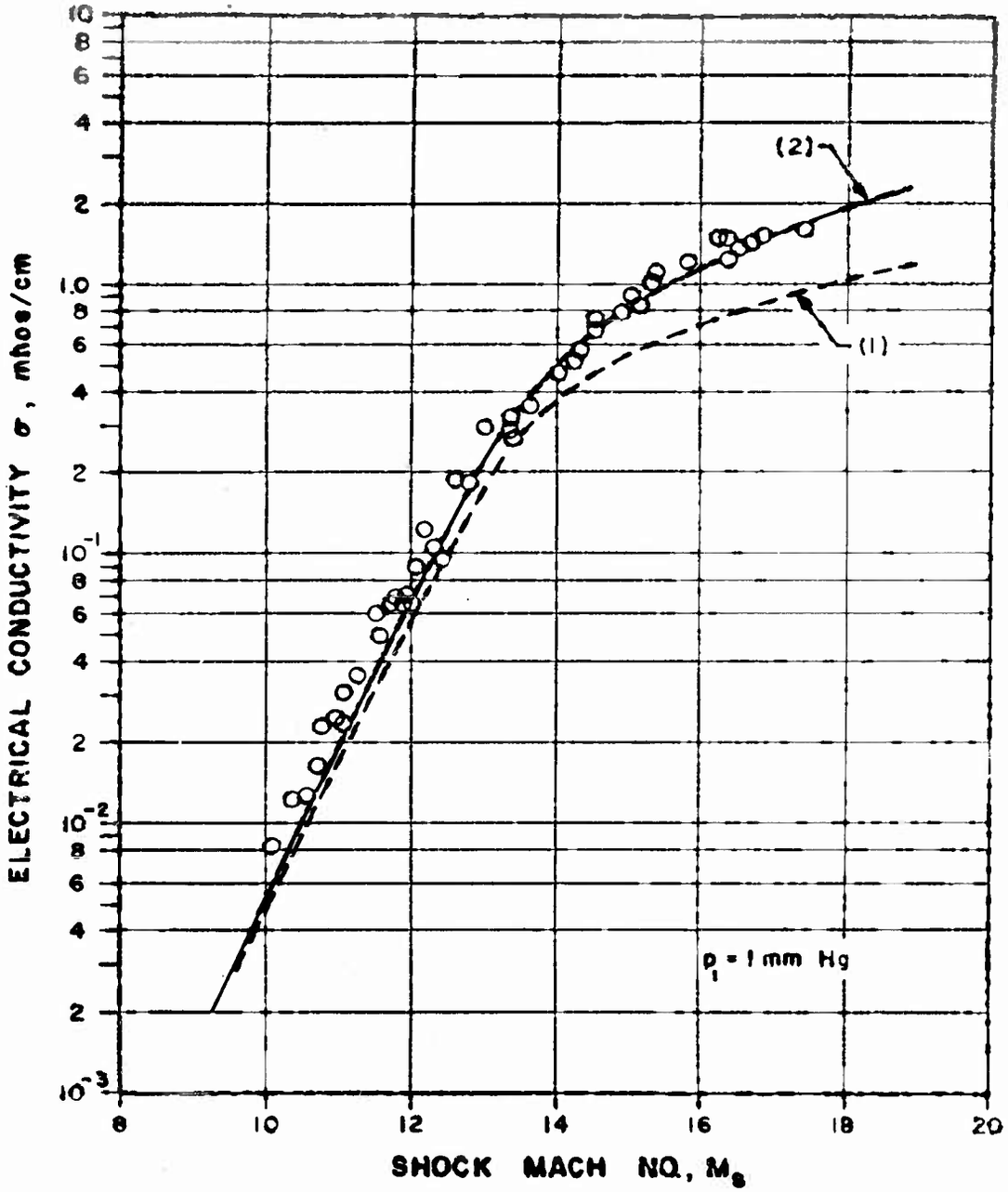

Fig. 21 — Comparison of measured electrical conductivity of shock-heated air with theory based on equilibrium degree of ionization, molecular cross sections and theoretical atomic cross sections.

(1) Atomic cross sections calculated from Ref. (18).

(2) Atomic cross sections calculated by Hammerling, Shine, and Kivel [19].

For this calculation it is necessary (and sufficient) to know the composition and density of the ionized gas, the electron temperature, and the average electron diffusion cross section of all species which contribute appreciably to the total electron collision probability. Since the results indicate thermodynamic equilibrium has been achieved in these experiments, the temperature, density and composition of the ionized gas at a given shock velocity and initial air density, and thus the concentrations of species which may contribute appreciably to the total electron cross section are known [7]. For the molecular species and for Argon the electron diffusion cross section is available in the literature [16]. For atomic oxygen and nitrogen, the electron diffusion cross sections have not been experimentally determined, and only somewhat contradictory theoretical estimates on the total electron collision cross sections of atomic oxygen seem to be available in the literature [17] [18]. Calculations have been made at this laboratory by Hammerling, Kivel and Shine [19] on the electron collision cross sections of oxygen and nitrogen atoms. The results are consistent with the measurements.

The electrical conductivities shown on Fig. (21), particularly in the strong shock region, are of an order of magnitude greater than the conductivity of sea water. As a result, the "thin" heat transfer gage must be insulated from the hot gas for very strong shocks by a thin layer, a fraction of a micron, of silicon monoxide.

Another product of this experiment is the indication that this experiment may possibly be used to determine the electron collision cross sections of individual species if the experiments are made in the component gases. It appears that even in measurements in a complex mixture such as air, cross sections calculated in Ref. (19) are clearly preferred over those calculated from simpler atomic models.

MAGNETOHYDRODYNAMICS

Work in high temperature gas dynamics and the exploitation of the shock tube as a research tool naturally lead us to the threshhold of magnetohydrodynamics. Until recently this field has been the private domain of the astrophysicists and those concerned with fusion reactors, but the interest of the aerodynamicist in the flow of partially ionized gases has injected new points of view.

The study of the interaction between magnetic fields and the flow of electrically conducting fluids covers a very wide range of physical phenomena from partially to completely ionized gases. At the AVCO Research Laboratory activities in both extremes of this area are in progress.

Research in the lower temperature, partially ionized gas regime, is aimed at exploiting the fundamental advantage offered by magnetohydrodynamics, i.e., being able to exert body forces on a fluid without any solid surface pushing on the fluid boundaries. Magnetohydrodynamics, therefore, changes the basic flow equations so as to open a new field in fluid dynamics. At the present state of development of this field, it is still impossible to foresee even its most important engineering applications [20] [21].

Experiments conducted at the AVCO Research Laboratory by Patrick, Brogan and Rosa [22] are designed to check the one-dimensional flow equations, including the effect of body forces due to the interactions between the conducting fluid and magnetic fields. This work can be done in ordinary shock tubes with gas thermally ionized by strong shock waves. It is a convenient simplification to close the current loops in the gas, eliminating the electrode problem and greatly simplifying analysis.

The principle of these experiments is to create an electric field due to the V x B interaction (velocity and magnetic field) in a direction perpendicular to both the magnetic field and the flow. In the schematic of the experimental arrangment shown in Fig. (22) this field closes a loop in the annulus. This current loop in turn produces a body force on the flow in a direction opposing the flow. The strength of the magnetic field is arranged so that the flow cannot be decelerated smoothly to sonic velocity by the body forces. As a result a standing shock must form in the field region, decelerate the flow to subsonic velocity and cause a loss in total pressure.

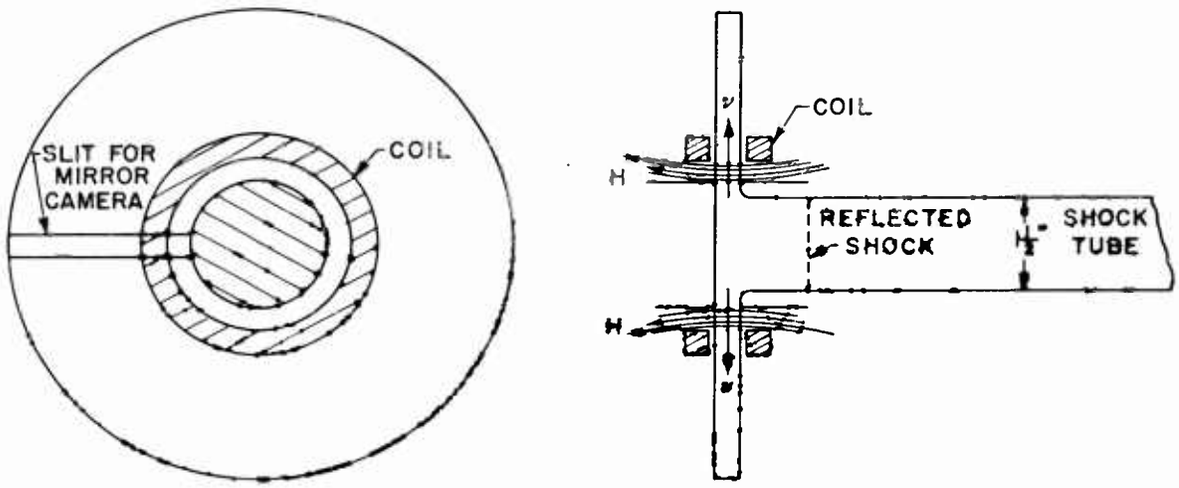

Fig. 22 — Geometry used for magnetic field-ionized gas interaction experiment. The hot, partially ionized gas behind the reflected shock flows through the field region, setting up an annular current which causes a body force to act on the flow opposite to the flow direction.

When the flow leaves the field region it expands (like the driver of a shock tube) but due to the total pressure loss in the standing shock, it does not recover the full velocity of the flow before interacting with the field. The change in flow velocity and the location of the standing shock can be calculated and compared with the experimental results. A mirror camera picture of the flow in the annulus under the action of the magnetic field is shown in Fig. (23) together with a schematic explanation of the process.

At the other extreme, in the fully ionized, low density gas regime efforts are being made to extrapolate our knowledge to conditions interesting to the astrophysicist and neuclear physicist. Producing new understanding in this region requires first a method of producing in the laboratory a controlled sample of this gas for study. Experiments performed at this laboratory to date by Janes and Petschek have achieved temperatures up to 400,000°K in the gas. Having created such a gas sample, the basic flow properties are now being studied.

The problem of producing this hot gas sample has been approached through use of essentially an electromagnetically driven shock tube. A changing magnetic field is used to accelerate an ionized mass of gas to a high velocity. The stationary cold gas ahead of the moving gas then has a high relative kinetic energy which is converted into thermal energy in a shock wave by collision with the moving gas and the magnetic field. Knowing the initial gas density and shock velocity, as in the conventional shock tube, the conditions behind the shock front can be calculated from the conservation laws.

One device which has been constructed for these experiments is illustrated schematically in Fig. (24) and shown in Fig. (25) in the illumination of its own light. The discharge of a high voltage capacitor through the primary coil causes current in the secondary split coil to produce an electrodeless ring discharge in the annular glass tube. This discharge is expelled down the tube by the magnetic field. Our capacitive power supply operating at 65 kv is capable of 10^{10} watts. In order to obtain temperatures of 10^6 °K it is necessary to accelerate deuterium, D_2, to a velocity of approximately 23 cm/μsec. Our velocity measurements to date have indicated temperatures of up to 4×10^5 °K (14 cm/μsec). D_2 is used because it can be raised to high stagnation temperatures with a minimum of energy.

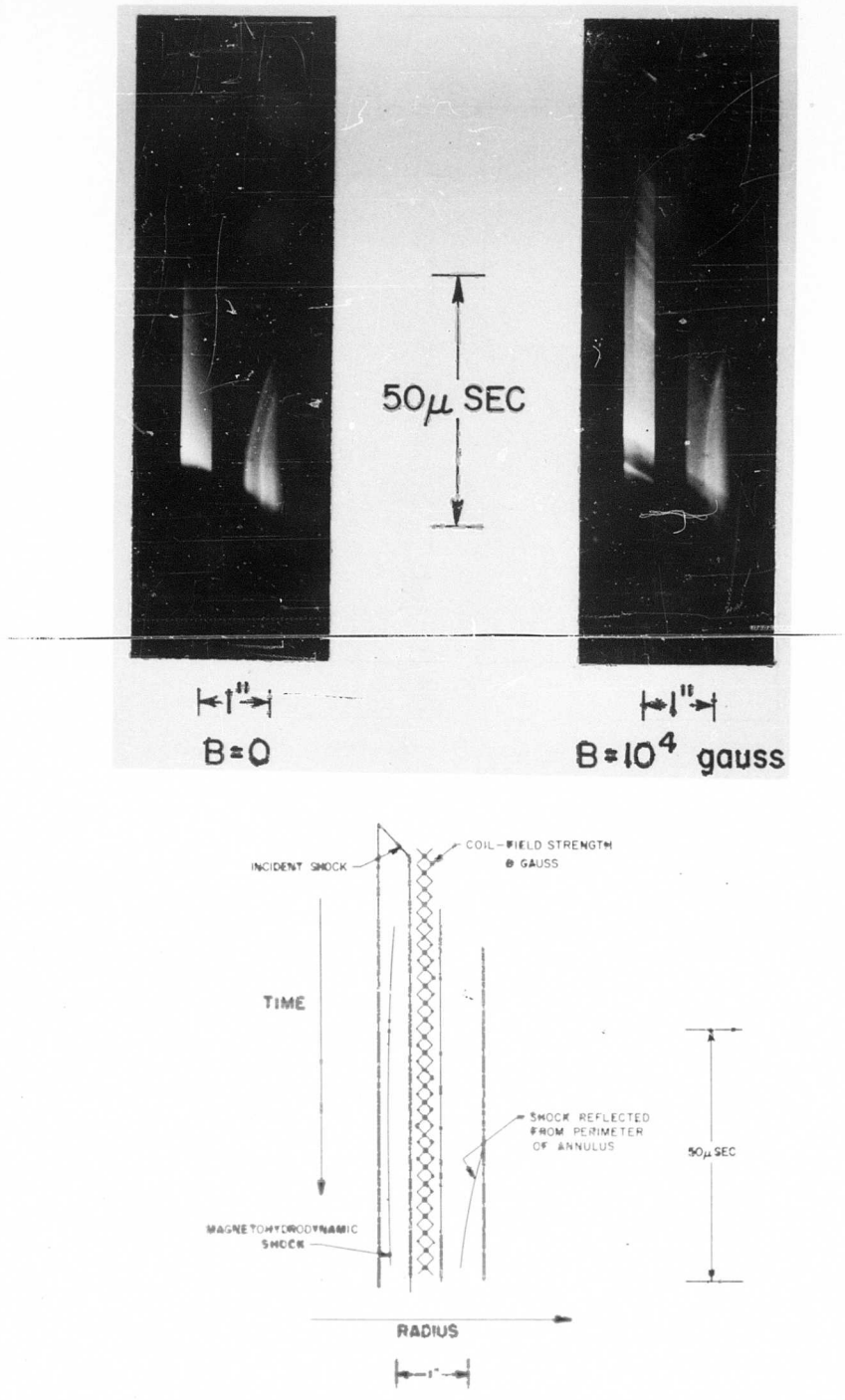

Fig. 23 — Mirror camera photograph of the luminosity in the flow (as seen through the slit shown in Fig. (22)) for experiments conducted without and with magnetic field applied. A schematic explanation of the important points is also shown for the experiment with field applied. Note the steady, standing shock in the field region.

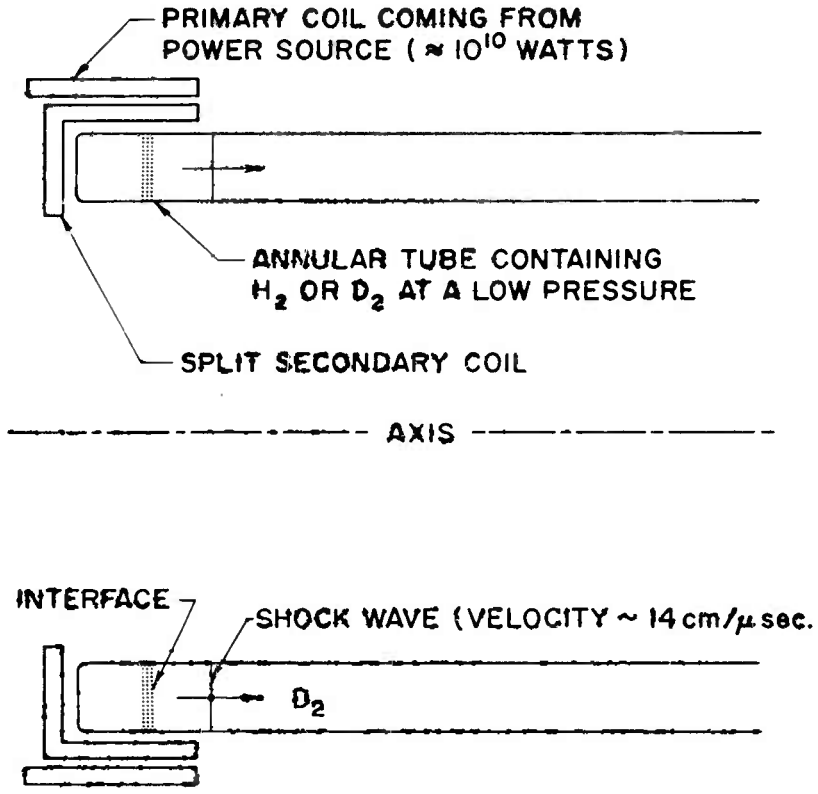

Fig. 24 — Simplified schematic sketch of one configuration of high temperature gas accelerator. (Power delivery system not shown).

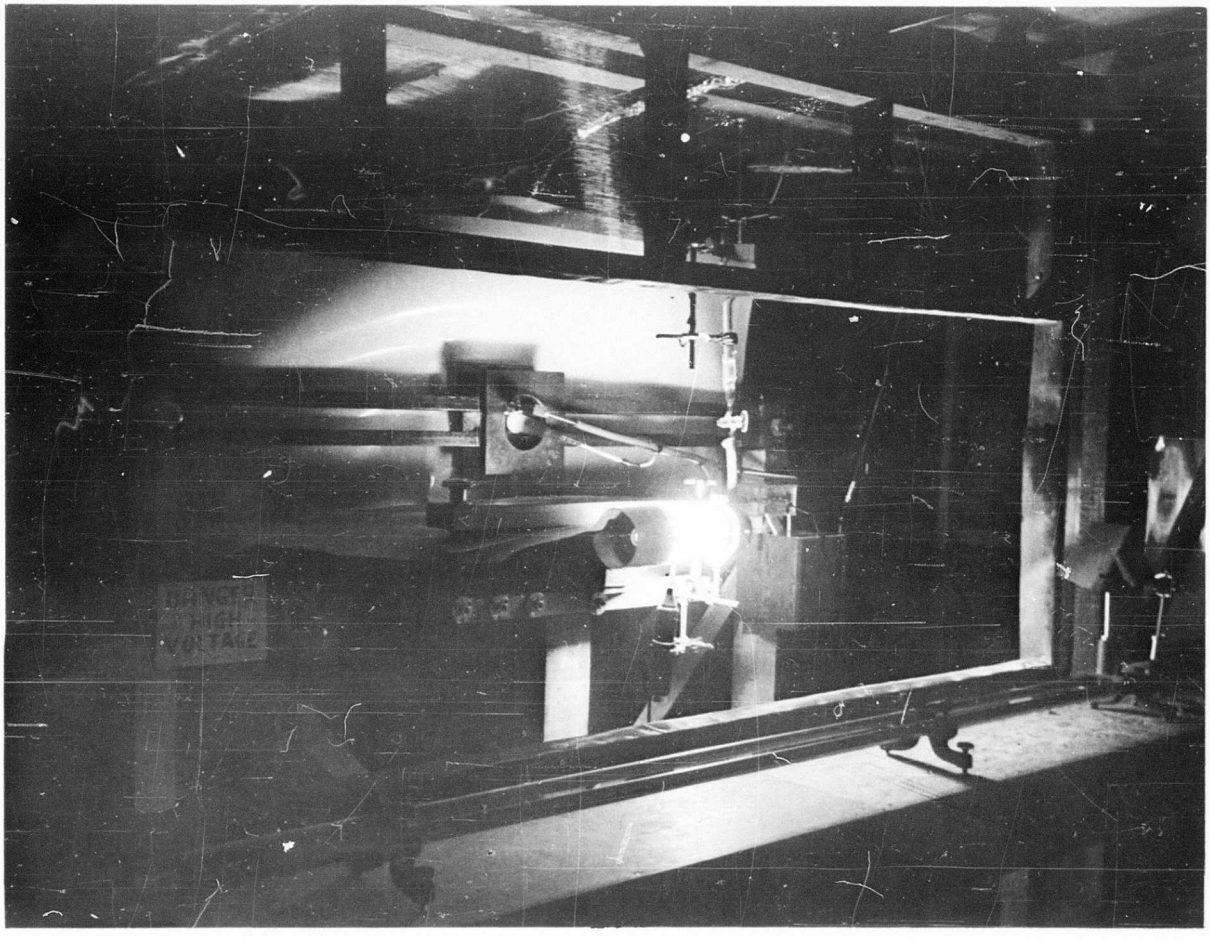

Fig. 25 — Photograph of the existing experimental arrangement illuminated by light from the annular discharge tube.

CONCLUDING REMARKS

The work discussed is representative of some of the work of the AVCO Research Laboratory during the past two years. It is typical of many other projects in which the laboratory is presently engaged and demonstrates the broad field of application for the shock tube in high temperature gas dynamics. It has been shown that the proper environment can be simulated to study many aspects of hypersonic flight problems. As an example of an aerodynamic problem, the heat transfer through the laminar boundary layer at the stagnation point has been discussed. A somewhat more physical phenomena, the emissivity of high temperature air, has been investigated and its role in hypersonic flight has been established. In addition, the electrical properties of high temperature air have been studied. In the analysis of all high temperature experiments, the chemical kinetics problem has been involved due to the dependence of the flow parameters on the thermochemical state of the gas. Experiments which have defined this state for the shock tube, and give order of magnitude answers for other situations, have been described. In addition, the preliminary results of our venture into magnetohydrodynamics, over a large temperature range, are presented. The scope of the work described shows the versatility of the shock tube as a research tool and the need for aerodynamicists to broaden their consideration to include new and previously unrelated fields in their attempt to understand the problems of hypersonic flight.

ACKNOWLEDGEMENT

Much of this work has been sponsored by the Western Development Division, Air Research and Development Command, U. S. Air Force, under Contract AF 04(645)-18.

REFERENCES

1. Dodge, J. A., "Ultra High Temperature Aerodynamic Testing Facilities," AGARD Memorandum AG 17/P7, Papers presented at the Sixth Meeting of the Wind Tunnel and Model Testing Panel, Paris, France, Nov. 1954.

2. Resler, E. L., Lin, S. C. and Kantrowitz, A. R., "The Production of High Temperature Gases in Shock Tubes," J. Appl. Phys. 23, 1390 (Dec. 1952).

3. Petschek, H., Rose, P. H., Glick, H. S., Kane, A. and Kantrowitz, A., "Spectroscopic Studies of Highly Ionized Argon by Shock Waves," J. Appl. Phys. 26, 83 (1955).

4. Lin, S. C., Resler, E. L. and Kantrowitz, A., "Electrical Conductivity of Highly Ionized Argon Produced by Shock Waves," J. Appl. Phys. 26, 95 (1955).

5. Rose, P. H. and Stark, W. I., "Stagnation Point Heat Transfer Measurements in Dissociated Air," AVCO Research Laboratory Research Note 24, Revised April, 1957.

6. Hilsenrath, J. and Beckettt, C., "Tables of Thermodynamic Properties of Argon-Free Air to 15,000°K," Arnold Engineering Development Center Report AEDC-TN-56-12, Sept. 1956.

7. Feldman, Saul, "Hypersonic Gas Dynamic Charts for Equilibrium Air," AVCO Research Laboratory, 1957.

8. Kantrowitz, Arthur, "Problems of High Mach Number Simulation," Talk given at Joint Session of Wind Tunnel Panel and Flight Test Panel, AGARD, Ottawa, Canada, June 1955.

9. Feldman, Saul, "The Chemical Kinetics of Air at High Temperatures: A Problem in Hypersonic Aerodynamics," AVCO Research Laboratory Research Note 25, Feb. 1957.

10. Fay, J. A. and Riddell, F. R., "Theory of Stagnation Point Heat Transfer in Dissociated Air," AVCO Research Laboratory Research Note 18, Revised April, 1957.

11. Cohen, C. B. and Reshotko, E., "Similar Solutions for the Compressible Laminar Boundary Layer with Heat Transfer and Pressure Gradient," NACA TN 3325, 1955.

12. Masson, D. J and Gazely, Carl, Jr., "Surface Protection and Cooling Systems for High Speed Flight," RAND Corporation Rept. P-829, Revised April, 1956.

13. Brown, H.K. and Rose, P.H., "Critical Analysis of Uncertainties Involved in Shock Tube Heat Transfer Measurements", AVCO Research Laboratory Research Note 30, (to be published).

14. Keck, J. C., Kivel, B. and Wentink, T., Jr., "Emissivity of High Temperature Air," AVCO Research Laboratory Research Note 33, April 1957.

15. Lin, S. C., "Electrical Conductivity of Thermally Ionized Air Produced in a Shock Tube," AVCO Research Laboratory Research Note 26, Feb. 1957. (Journal of Applied Physics, July, 1957).

16. Massey, H.S.W. and Burhop, E.H.S. "Electronic and Ionic Impact Phenomena," New York, Oxford University Press. 1952.

17. Mitra, S.K., Ray, B.B. and Ghosh, S.P., "Cross Section of Atomic Oxygen for Elastic Collision with Electrons, and Region of F Absorption," Nature, 145, 1017 (1940).

18. Yamanouchi, T., "Progress of Theoretical Physics", Vol. II, 1947, p. 23.

19. Hammerling, P., Shine, W. and Kivel, B., "Low Energy Elastic Scattering of Electrons by Oxygen and Nitrogen," AVCO Research Laboratory Research Note 31, March, 1957.

20. Rosa, Richard, "Shock Wave Spectroscopy and Engineering Magnetohydrodynamics," Ph.D. Thesis, Cornell University, 1956.

21. Patrick, Richard, "Magnetohydrodynamics of Compressible Fluids," Ph.D. Thesis, Cornell University, 1956.

22. Patrick, R. M. and Brogan, T., "One-dimensional Flow of an Ionized Gas through a Magnetic Field," AVCO Research Laboratory Research Note 36, (to be published).

23. Logan, J. G., "Relaxation Phenomena in Hypersonic Aerodynamics," Paper presented at 25th Annual Meeting of the Institute of Aeronautical Sciences, New York, Jan. 1957.

24. Glick, H. S. and Wurster, W., "Shock Tube Study of Relaxation Phenemena in Oxygen," Paper presented at Meeting of American Physical Society, New York, Jan. 1957.

25. Camm, J. and Keck, J. C., "Radiative Relaxation Behind a Shock Wave," Paper presented before American Physical Society, Washington, D. C., April, 1957.

26. Blackman, V. H., "Vibrational Relaxation in O_2 and N_2," Technical Report II-20, Princeton University, May, 1955.

27. Kivel, B., Mayer, H. and Bethe, H., "Emissivity of Nitric Oxide in High Temperature Air," To be published in Annals of Physics, July, 1957.

28. Gilmore, F. J., "Equilibrium Composition and Thermodynamic Properties of Air at 24,000°K," RAND Corporation, RM-1543, August, 1955.

29. Logan, J. G. and Treanor, C. E., "Thermodynamic Properties of Air between 3000°K and 10,000°K," Cornell Aeronautical Laboratory Report No. BE-1007-A-3, April, 1957.

30. Kemp, N. J. and Riddell, F. R., "Heat Transfer to Satellite Vehicles Re-entering the Atmosphere," AVCO Research Laboratory Research Note 21, Oct. 1956, (Published in Jet Propulsion, 27, 132, Feb. 1957).

31. Chaibai, A. J. and Emrich, R. J., "Measurement of Wall Temperature and Heat Flow in the Shock Tube," Journal of Applied Physics, 26 (June, 1955), p. 779.

32. Vidal, R. J., "Model Instrumentation Techniques for Heat Transfer and Force Measurements in a Hypersonic Shock Tunnel," Cornell Aeronautical Laboratory Report No. AD-917-A-1, Feb. 1956.

UNCLASSIFIED